# ENCLOSURE 2

# MFN 15-056

# Responses to NRC RAIs for NEDC-33376P, Revision 1 and NEDC-33377P, Revision 1 Submittal

# Non-Proprietary Information - Class I (Public)

**IMPORTANT NOTICE**

This is a non-proprietary version of Enclosure 1, from which has the proprietary information has been removed. Portions of the enclosure that have been removed are indicated by an open and closed bracket as shown here [[ ]].

# MODEL DESCRIPTION NEDC-33376P, REVISION 1 RAIs

## RAI 1: Range of Applicability

1-1. Please provide more specific details regarding the range of application of LANCR02. To this end, please specify any limits on the following parameters:

- The range of beginning of life (BOL) uranium enrichment
- The range of BOL plutonium concentration
- The range of BOL gadolinia concentration
- The range of in-channel void fraction
- The range of inactive flow channel void fraction (e.g. bypass)
- The range of channel bow

1-2. Please also specify any inherent limitations of the LANCR02 methodology that would preclude the application of this method to particular analyses. As an example, the code may presume symmetry of the lattice along particular dimensions, and as a consequence may not be applicable to non-symmetric fuel designs.

1-3. Please provide the functions and restrictions for LANCR02 that are specified in the user manual.

1-4. Lattices have been proposed that include control blade spans that exceed one fuel bundle. Is it the intent to seek approval of LANCR02 to analyze such lattices?

## GNF Response to RAI 1

1-1. There are no inherent limitations on the variables specified that preclude the LANCR02 models from analyzing problems in which these variables assume any value within their full physically realizable range. Modeling limitations, regarding the range of application, on the BOL uranium enrichment, BOL plutonium concentration, BOL gadolinia concentration, in-channel void fraction, inactive flow channel void fraction, and the channel bow are identified in the following list. Limits on several parameters with respect to the application of LANCR02 are provided in RAI 1-3.

- There is no modeling limitation on BOL uranium enrichment.
- The ability to model high Pu concentration accurately is limited by the use of the transport corrected P0 cross section library and the quadrature set. However, the low plutonium concentrations present in MOX fuel is within the range of applicability of the chosen cross section library and quadrature set. More detail on the range of Pu concentration is included in request for additional information (RAI) responses 1-2 and 1-3.
- There is no modeling limitation on BOL gadolinia concentration.
- There is no modeling limitation on in-channel void fraction.
- There is no modeling limitation on inactive flow channel void fraction.
- There is no modeling limitation on channel bow.

1-2. The inherent limitations of the LANCR02 methodology, within the context of the light water reactor fuel assembly modeling application, are:

- Problems in which transport corrected P0 cross sections do not apply.
- Hexagonal geometry

1-3. The following functions and restrictions for LANCR02 are specified in the user manual. These restrictions do not imply modeling limitations, but are provided for guidance to the user with respect to the range of application.

Functions

- [[

]]

Modeling Capabilities

- [[

]]

Restrictions

- [[

]]

1-4. No, it is not the intent to seek approval of LANCR02 to analyze lattices that include control blade spans that exceed one fuel bundle. However, we would consider this a geometry modification that would be allowed per Section 9.

**RAI 2: Items in the Cross-section Libraries**

2-1. Please clarify what is meant by the following identifiers in Table A-2:

- PSD-1
- PSD-2
- Act_resd
- FP_resd
- Energy

2-2. Please specify how the "H2O" and "D2O" cross-sections were generated. Do these cross-sections consider chemical binding effects?

Please incorporate this information in a revision to the LANCR02 Model Description LTR.

**GNF Response to RAI 2**

2-1. PSD-1 is the sum of all fission products that are not explicitly tracked in the library. PSD-2 is the same as PFP2 in Figures 5-1 to 5-4. Table A-2 of the Model Description licensing topical report (LTR) will be revised to change "PSD-1" and "PSD-2" to "PFP1" and "PFP2", respectively. In addition, definitions of PFP1 and PFP2 will be added to the Model Description LTR Section 5.7.

Act_resd, FP_resd, and Energy are internal arrays in LANCR02. The Model Description LTR will be updated to remove these entries from Table A-2.

2-2. All H2O and D2O cross sections except the scattering cross section are created by assuming H2O and D2O are isotopic mixtures of O, H and D isotopes, respectively. For H2O and D2O scattering cross sections, the chemical binding effects are accounted for with the LEAPR module of NJOY99. LEAPR accounts for the change in coherent and incoherent elastic scattering data in bound material moderators. All other reactions are unchanged by LEAPR and continue to be treated as "free-gas" materials.

**RAI 3: Gamma Cross Sections**

3-1. Please specify the source of the gamma cross sections.

3-2. Please specify the source of the fission and capture gamma spectra. Please incorporate this information in a revision to the model description LTR.

**GNF Response to RAI 3**

3-1. Appendix B of the LTR will be revised to include the following information:

The energy boundaries of the final 8-group energy structure are shown in Table B-1. Because the 8-group energy structure is too coarse to be generated directly from continuous energy cross section data, the library was generated using a two-step process.

First, an 80-group energy structure was defined spanning Table B-1, in which each of the 8 energy groups listed in Table B-1 were further sub-divided into 10 groups of equal energy widths. Gamma cross sections were evaluated for each element at each midpoint energy of the 80-groups.

A processing code was used to create 80-group gamma cross sections. In this code, continuous energy gamma cross sections are expressed by formulae based on combined experimental and theoretical data. The sources of the gamma cross sections are the various expressions given in NEDE-23695. Section III.2 and the supporting Table 3.1 from NEDE-23695 are included herein. Because energy variations of gamma cross sections are relatively smooth, a cross section value at the midpoint energies of each 80-group may be taken as the simple average over a group. The resulting gamma cross sections were assumed to be independent over conditions of interest.

The gamma spectrum is affected mainly by heavy elements and is insensitive to the void fraction. Therefore, the gamma spectrum in a boiling water reactor (BWR) remains nearly the same over the commercial BWR fuel bundles from the old to new designs. This fact validates the use of typical gamma spectrum to condense 80-group cross sections into fewer 8 energy groups.

Based on the 80-group cross sections, a single fuel pin cell transport calculation was performed using ANISN (1-D cylinder, isotropic scattering, S8) (Reference 3-1). The resulting gamma spectrum was used as a weighting function to condense cross sections into the target 8-group energy structure. The final 8-group cross section data has been loaded into a file.

During this processing, an energy deposition cross section was defined as,

$$\sigma_e^{\gamma} = \frac{\sum_{\Gamma \in \gamma} \phi_{\Gamma} \left\{ E_{\Gamma} \sigma_{PE+PC}^{\Gamma} + \sum_{\Gamma' \geq \Gamma} \left( E_{\Gamma} - E_{\Gamma'} \right) \sigma_{CS}^{\Gamma \to \Gamma'} \right\}}{\sum_{\Gamma \in \gamma} \phi_{\Gamma}}$$

where, $\gamma$ and $\Gamma$ represent the 8-group and 80-group energy structures, respectively; $\phi_{\Gamma}$ is the 80-group gamma flux; $E_{\Gamma}$ is a midpoint energy of group $\Gamma$; $\sigma_{PE+PC}^{\Gamma}$ is the sum of the photoelectric and pair creation cross section in the 80-group energy structure; and $\sigma_{CS}^{\Gamma\rightarrow\Gamma'}$ is the Compton scattering cross section in the 80-group energy structure.

3-2. The source of the fission and capture gamma spectra is ENDF/B-V for the main nuclides (U-235, U-238, Pu-239, Pu-240). The data sources for all other nuclides come from older data sources like ENDF/B-IV, JENDL-1, and JENDL-2, depending on the availability of data for each particular nuclide.

**Reference**

3-1 W. W. Engle, Jr., “ANISN, A One-Dimensional Discrete Ordinates Transport Code with Anisotropic Scattering,” ORGDP Report K-1693, Oak Ridge, TN (1967).

[[

]]

[[

]]

[[

]]

[[

]]

[[

]]

[[

]]

[[

]]

[[

]]

[[

]]

**RAI 4: NJOY Broadened Libraries**

The staff requires additional details regarding the generation of the temperature dependent 118 group libraries.

4-1. Please specify the standard production temperatures that are used in NJOY to broaden the evaluated nuclear data file (ENDF) cross-sections.

4-2. Describe the process for fitting the f-tables to NJOY output. Please incorporate this information in a revision to the model description LTR.

**GNF Response to RAI 4**

4-1. All isotopes except D2O, H2O, H and H2 are evaluated in NJOY at ten temperature points: 293K, 373K, 559K, 748K, 793K, 833K, 963K, 1273K, 1773K and 2573K. D2O, H2O, H and H2 are evaluated at 293.6K, 350K, 400K, 450K, 500K, 550K and 600K. D2O and H2 are additionally evaluated at 650K while H2O and H are additionally evaluated at 800K.

4-2. F-tables are ratios of the NJOY processed self-shielded cross sections at different temperatures and background cross sections to the base NJOY cross sections defined as the infinitely diluted cross section at 293K.

For each isotope, reaction, group, and temperature, an F-table entry is constructed with NJOY data using the definition:

$$f^{g}_{x,iso}(T,\sigma_0) = \frac{\sigma^{g}_{x,iso}(T,\sigma_0)}{\sigma^{g}_{x,iso}(293K,\infty)}$$

This operation is performed (library preprocessing) for a number of temperatures (see 4-1) and background cross sections (e.g., 1E+10, 1E+6, 1E+5, 1E+4, 1E+3, and 1E+2 barns), depending on the type of isotope, forming a discrete two-dimensional table for every cross section type per isotope. For a given cross section at a specific temperature and background cross section, the corresponding two-dimensional f-table is then interpolated to extract the correct cross section according to Equation (3) of the LTR.

*In order to remove confusion caused by the wording of the LTR, the paragraph preceding and including Eq. (3) of the LTR will be replaced by the following:*

For each isotope in the LANCR02 cross section library, the NR approximation is used to create a base cross section set at 293K for infinitely dilute conditions by setting $\sigma_0$ equal to a very large value in Eq. (2) (i.e., $\sigma_0 >> \sigma_{t,iso}(E)$, representing a resonance absorber present in such small abundance that the resonances do not affect the flux spectrum).

For each isotope iso, reaction x, group g, temperature T, and background cross section $\sigma_0$ an f-table is constructed with NJOY data using the definition:

$$f^{g}_{x,iso}(T,\sigma_0) = \frac{\sigma^{g}_{x,iso}(T,\sigma_0)}{\sigma^{g}_{x,iso}(293K,\infty)}$$

This operation is performed (library preprocessing) for a number of temperatures (e.g., 293K, 373K, 559K, 748K, 793K, 833K, 963K, 1273K, 1773K and 2573K) and background cross sections (e.g., 1E+10, 1E+6, 1E+5, 1E+4, 1E+3, and 1E+2 barns), depending on the type of isotope, forming a discrete two-dimensional table for every cross section type per isotope. For a given cross section at a specific temperature and background cross section, the corresponding two-dimensional f-table is then interpolated to extract the correct cross section according to:

$$\sigma^{g}_{x,iso}(T,\sigma_0) = \sigma^{g}_{x,iso}(293K,\infty)\cdot f^{g}_{x,iso}(T,\sigma_0) \quad (3)$$

**RAI 5: Energy Boundaries of the Group Structures**

5-1. Verify that 1.0E-5 electron-volts (eV) are the lower boundary of the final group structure in Table A-4.

5-2. Please clarify the [[
]] mentioned below Table A-4?

5-3. Verify that 1.1175E+05eV is the lower boundary of the eighth group in Table B-1.

**GNF Response to RAI 5**

5-1. 1.0E-5 eV is the lower boundary of the lowest energy group in the library. Table A-4 in the Model Description LTR will be revised to clarify that 1.0E-5 is the lower boundary of the neutron library.

5-2. [[

]]

5-3. The lower boundary of the eighth gamma group in Table B-1 should be 1.175E+05 eV (not 1.1175E+05). Table B-1 in the Model Description LTR will be revised to show that 1.175E+05 eV is the lower boundary of the gamma library.

**RAI 6: Thermal Microscopic Neutron Cross-section Processing**

6-1. Please describe any features of the process for generating fine group cross-sections in the thermal energy range that account for differences in the neutron flux spectrum at low energies.

6-2. Does LANCR02 accept coolant temperature as an input?

6-3. If so, where and how is this information utilized in the cross-section generation process?

Please incorporate this information in a revision to the LANCR02 Model Description LTR.

**GNF Response to RAI 6**

6-1. The fine-group cross sections used in the pin cell calculation are evaluated as functions of temperature and background cross section. The chemical binding effects at low energies have are already accounted for in the fine-group neutron library (see RAI 2-2). The neutron flux spectrum is accounted for with the multigroup energy structure and there are no special models in LANCR02 for low energies.

6-2. Coolant and moderator temperatures are input parameters in the LANCR02 input file.

6-3. The coolant temperature is used to interpolate the temperature dependent cross sections at the user defined statepoint.

No modifications to the Model Description LTR are needed.

**RAI 7: Background Cross Section Calculation**

7-1. Please provide additional information regarding the determination of an acceptable Bell factor.

7-2. Are the Bell factors determined from Monte Carlo N-Particle (MCNP) calculations?

7-3. If so, how are the Bell factors deemed appropriate for problem-specific application if a set of pre-determined Bell factors are used for standard production purposes?

Please incorporate this information in a revision to the model description LTR.

**GNF Response to RAI 7**

7-1. The goal of using the LANCR02 Bell factor is to obtain single-pin background cross sections for appropriate cross section selection of each resonance absorber isotope in each fuel mixture in the lattice. The surface component of the macroscopic background cross section for a single fuel region or for the generalization to subregions within the fuel lump (e.g., Gd pins) uses the LANCR02 Bell factor. The current acceptability criteria for an enhanced Bell factor is based on the overall comparison of LANCR02 results to MCNP values presented in the qualification licensing topical report. The method is simple because it does not use a numerical solution to the effective resonance integral for neutron escape because that would be computationally costly (see Reference 7-1).

Information regarding the determination of the acceptable Bell factor for LANCR02 is provided below.

Section 2.2.1 of the Methodology LTR will be revised to include the following:

The LANCR02 Bell factor is a sensitive function mildly dependent on fuel temperatures and pellet radii, centered on values that are typical to a Light Water Reactor. Although the adjusted Bell factor is relatively close to the Bell recommended value (e.g., 1.16, Reference 7-2), it provides flexibility for customization to LWR fuel lattice and temperature conditions.

[[

]]

[[

]]

**Figure 2-1: Comparison of the Escape Probability Approximated with a Bell Factor to a Two-Term Carlvik Rational Approximation**

7-2. The Bell factors are not determined from Monte Carlo N-Particle (MCNP) calculations. It is a parametric functional with weak dependency on pellet radius and fuel temperature. That is, it is not based on a MCNP single-rod study. The choice of Bell factor was based on the classical approach of Reference 7-2 and validated by comparison to MCNP results.

7-3. The same Bell factor treatment is used for all production cases. The adequacy of the Bell factor for problem-specific application is demonstrated in the acceptability of the results of the LANCR02 Qualification LTR.

**References**

7-1 "Accuracy of the Wigner Approximation", Y. G. Pashkin, Atomic Energy, Vol. 28, No. 2, 1970.

7-2 "Methods of Steady-State Reactor Physics in Nuclear Design," R. J .J. Stamm'ler, M. J. Abbate, Academic Press, 1983.

**RAI 8: Isolated Pin Flux Calculation**

8-1. When performing the isolated pin flux calculation to determine the Dancoff factor, how is the calculation performed?

8-2. Please describe the problem size and specify the boundary conditions that are applied.

**GNF Response to RAI 8**

8-1. When performing the isolated pin flux calculation to determine the Dancoff factor, a square 5x5 array of cells is constructed for each representative fuel pin, including non-fuel structures inside the channel, each square cell of the array having the dimension of the fuel pin pitch. The "isolated" pin being evaluated is placed at the center of this lattice, and all non-fuel regions within the pin cell are given a constant source with the constraint that the source is directly proportional to the cross section, as derived in Reference 6 of the Methodology LTR. The boundary of the array is reflective, as is the case during a typical transport solution using the current implementation of the Method of Characteristics. Each of the 24 pins that are not the fuel pin are filled with moderator, and given a constant source, as described in Section 2.2.2 of the Methodology LTR and in Reference 6 of the Methodology LTR. The isolated fuel pin flux, $\phi_0$, used in the Dancoff factor calculation of Equation (12) is then the flux calculated for the geometry described within the region being evaluated (i.e., fuel, cladding, or non-fuel region).

Reference 6 of the Methodology LTR describes in more detail how the isolated fuel pin flux calculation is performed for the Dancoff factor calculation.

8-2. The isolated pin flux calculation used to determine the Dancoff factor uses a square 5x5 array of cells, each square cell of the array having the dimension of the fuel pin pitch. A reflective boundary condition is applied at the boundary of the array.

Reference 6 of the Methodology LTR and RAI 8-1 response describe in more detail how the isolated fuel pin flux calculation is performed for the Dancoff factor calculation.

**RAI 9: Dancoff Factor Calculation for Non-Fuel Pin Regions**

The discussion regarding the calculation of the Dancoff factors for non-fuel pin regions is not sufficiently detailed for the NRC staff to review this method.

9-1. Please provide a more detailed description of the calculation of the Dancoff factors for these other regions.

9-2. Please comment on the validity of [[
]].

**GNF Response to RAI 9**

9-1. Dancoff factors are traditionally employed in fuel pins as a correction factor to the resonance escape probability to account for the shadowing effect of neighboring fuel pins. The resonance escape probability is needed to calculate the correct resonance cross sections for fuel isotopes. Resonance calculations for non-fuel isotopes have traditionally not been included because the resonance effect of non-fuel isotopes is smaller. However, to improve the results in cladding and channel materials, LANCR02 includes a resonance calculation for zirconium cross sections. Because zirconium is not part of the fuel regions, traditional methods that rely on circular fuel pin geometry cannot be used. Instead, the method of calculating Dancoff factors in complicated geometries as described in Reference 6 of the Methodology LTR is used. Reference 6 of the Methodology LTR contains a detailed description of the methodology.

9-2. [[

]]

**RAI 10: Ultra-fine Group Calculation**

The staff requires additional descriptive details of the ultra-fine group structure.

10-1. How are the ultra-fine group-wise cross sections determined from the continuous cross sections?

10-2. Are there a set number of ultra-fine groups used for this analysis, or is it determined on a case specific basis?

**GNF Response to RAI 10**

The Resonance Interference (RIF) model is not currently used in production cases and is not used in any of the results contained in the LANCR02 Qualification LTR. Therefore, we are not requesting Nuclear Regulatory Commission (NRC) approval of this methodology at this time, and the Methodology LTR will be modified to redact this description (Section 2.3).

**RAI 11: Resonance Interference Effects**

The Model Description LTR describes an ultra-fine group spectrum calculation that is performed to account for resonance interference effects utilizing the narrow resonance (NR) approximation. The LTR states that this approximation is less accurate below 50 eV. The staff would expect that at lower epithermal energies (1-10 eV) strong low-lying resonances may be inaccurately treated in the current method.

11-1. Comment on the accuracy of this method to predict plutonium-240 absorption. Please specifically address the absorption resonance at 1.056 eV.

11-2. The staff anticipates that LANCR02 depletion calculations will be performed at high instantaneous and historical void conditions (such as 100 percent in-channel void). Please discuss any consequences of high void depletion modeling given potential inaccuracies in the treatment of strong low-lying resonances. Specifically address gadolinium and plutonium.

**GNF Response to RAI 11**

The RIF model is not currently used in production cases and is not used in any of the results contained in the LANCR02 Qualification LTR. Therefore, we are not requesting NRC approval of this methodology at this time, and the Methodology LTR will be modified to redact this description (Section 2.3).

**RAI 12: Sub-Bundle Void Distribution**

12-1. Please confirm that the sub-bundle void distribution model is fully consistent with the previously approved void distribution model in TGBLA06. Please provide a direct comparison between pin-wise void fractions generated by TGBLA06 and LANCR02.

12-2. If there are any deviations, please note these deviations and justify them.

**GNF Response to RAI 12**

12-1. The correlation used in the sub-bundle void distribution model in LANCR02 is fully consistent with the previously approved void distribution correlation in TGBLA06. The only difference between the void distribution models in the two codes is the implementation.

The inherent difference in pin powers between TGBLA06 and LANCR02 complicates the direct comparison of the void fractions from the in-channel void distribution models in the two codes. A quantification of the calculated pin power differences can be demonstrated by comparing the relative pin power root mean square (RMS) values for uniform void distributions between the two codes for a single representative lattice. For this lattice, the relative pin power RMS values are [[ ]] and [[ ]] for uncontrolled and controlled cases respectively.

The difference in void fractions from the in-channel void distribution models in the two codes is shown in Table 12-1 and Table 12-2. The corresponding void fraction RMS values are [[ ]] and [[ ]] while the relative power RMS values are [[ ]] and [[ ]] for the uncontrolled and controlled cases respectively. This slight increase in relative power RMS values is attributed to the interplay between the in-channel void fractions and the pin powers.

A summary of the RMS value comparisons is provided in Table 12-3 for uncontrolled states and Table 12-4 for controlled states.

**Table 12-1: Void Fraction Differences Between TGBLA06 and LANCR02 for an Uncontrolled Case**

| | | | | | | | | | |
|---|---|---|---|---|---|---|---|---|---|
| [[ | | | | | | | | | |
| | | | | | | | | | |
| | | | | | | | | | |
| | | | | | | | | | |
| | | | | | | | | | |
| | | | | | | | | | |
| | | | | | | | | | |
| | | | | | | | | | |
| | | | | | | | | | |
| | | | | | | | | | ]] |

**Table 12-2: Void Fraction Differences Between TGBLA06 and LANCR02 for a Controlled Case**

| | | | | | | | | | |
|---|---|---|---|---|---|---|---|---|---|
| [[ | | | | | | | | | |
| | | | | | | | | | |
| | | | | | | | | | |
| | | | | | | | | | |
| | | | | | | | | | |
| | | | | | | | | | |
| | | | | | | | | | |
| | | | | | | | | | |
| | | | | | | | | | |
| | | | | | | | | | ]] |

**Table 12-3: Summary of Uncontrolled Comparisons between TGBLA06 and LANCR02 Evaluations**

| | RMS (%) |
|---|---|
| In-channel Void Distribution Differences | [[ |
| Pin Power Differences (uniform void) | |
| Pin Power Differences (distributed void) | ]] |

**Table 12-4: Summary of Controlled Comparisons between TGBLA06 and LANCR02 Evaluations**

| | RMS (%) |
|---|---|
| In-channel Void Distribution Differences | [[ |
| Pin Power Differences (uniform void) | |
| Pin Power Differences (distributed void) | ]] |

12-2. [[

]]

**RAI 13: Buffer Zone**

Please discuss the rationale behind treating the buffer zone based on lattice average quantities as opposed to nearest neighbors.

**GNF Response to RAI 13**

The nearest neighbor approach produces a reasonable approximation to the actual leakage spectrum if the neutron mean free path does not extend beyond the neighboring cells due to heavy moderation. However, at voided conditions, a neutron mean-free-path can be large and the leakage spectrum for each pin can be affected by distant cells in the lattice. Both methods give reasonable results.

The lattice average buffer zone can better account for lattice-wide effects such as control blades and vanished pins, especially at high void conditions. This approach can give a better fission source to drive the transport solution and can produce a better representation of the actual spectrum, particularly for pins with low reactivity (gad).

LANCR02 is not as sensitive to the pin cell calculations as other methods. LANCR02 only uses the pin cell calculations to condense the flux spectrum from a fine to intermediate energy group structure and a full transport solution is performed without any homogenization at the pin cell level.

**RAI 14: Gas Gap**

14-1. Please describe at what stages in the flux condensation calculations and in the lattice spatial flux distribution calculations that the gas gap is considered.

14-2. Please address equation (7) in terms of the source of the geometric data (cladding inner diameter or fuel pellet outer diameter).

14-3. Please provide clarifying text to accompany Figure 2-1. Specifically, is the gap treated as part of the cladding or fuel region, or neglected?

14-4. Please clarify Figures 7-1, 7-2, and 7-3 in terms of the treatment of the gas gap.

14-5. Please list and justify any assumptions made in the calculation regarding the gas gap.

Please incorporate this information in a revision to the model description LTR.

**GNF Response to RAI 14**

14-1. The gas gap is never modeled explicitly in LANCR02. The volume of the gap region is filled immediately at the beginning of the LANCR02 calculation with material from the fuel, and the density of the fuel pellet is modified to preserve mass.

14-2. Equation (7) refers to the fuel pellet outer diameter, which has been smeared to include the gap. Therefore, this is the cladding inner diameter. The text directly following Equation (7) will be modified as

"where V refers to the volume of the fuel pellet; S refers to the pellet surface area; and r is the pellet radius. In this case, the 'fuel pellet' has been smeared across the pellet/cladding gap, and the geometric volume, surface area, and the pellet radius therefore correspond to the inner cladding radius."

14-3. Figure 2-1 is not meant to show the exact geometry of the fuel pin, gas gap, and clad. Instead, the purpose of the figure is to show how a "Buffer Zone" is used to model the effects of fuel pins surrounding an isolated fuel pin during the pin cell spectral calculation. The gap is treated as part of the fuel pin, which is smeared to include the gap.

14-4. Figures 7-1, 7-2, and 7-3 are only meant to show configurations, listed in Table 7-1, that may be analyzed with the LANCR02 methodology. The gas gap of Figure 7.1 is not modeled explicitly. As described in this RAI response, the fuel is "smeared" over the gap region, and the fuel pellet density is modified to preserve mass. Figure 7.2 shows the geometry that may be modeled for this particular configuration (i.e., square lattice of fuel pins without channel box). In this figure, the fuel pellet has been "smeared" over the gap region. Figure 7.3 shows the geometry that may be modeled for this particular configuration (i.e., full fuel assembly with channel box and optional control blade). The detail of the cladding is not shown in this figure, although it is modeled explicitly.

14-5. The gas gap is filled with fuel, as described above, and the fuel density is reduced as necessary to preserve fuel mass. This approximation is justified first by the fact that,

during normal operation, the fuel expands to fill the pellet-clad gap. Additionally, if the fuel is assumed not to swell to fill the pellet-clad gap, the error introduced in this slight redistribution of mass is insignificant.

**RAI 15: Pin-Cell Calculations for Non-Fuel Pins**

The pin-cell calculations appear to require a cylindrical geometry similar to a fuel pin.

15-1. Please provide a description of how the pin-cell spectra are calculated for non-fuel pins, such as water rods and the water gap.

15-2. Please also provide additional details regarding the pin-cell calculations for plena. These details should include a discussion of any features that address the very low density of the gas.

**GNF Response to RAI 15**

15-1. The one-dimensional pin cell spectral calculation methodology is described generally in Section 2.3.1 of the Methodology LTR. More detail on how the method is applied to various types of non-fuel pins is provided here.

Small water rods
The water rod pin cell spectrum is calculated the same way as a fuel pin, as described in Section 2.3.1 of the Methodology LTR, except that moderator material is placed in the fuel region.

Large water rods
The water box, diamond, and large water rods (water rods, boxes and diamonds occupying more than one pin cell), are converted to an array of equivalent small water rods, collectively occupying the same volume as the actual structure modeled (for example, a 10x10 lattice's water box may occupy 9 fuel pin locations), where the water rods of the array preserve the volume of constituent materials. The pin cell spectrum of each pin cell of the array is calculated the same way as for a small water rod.

Inner water gaps and channel box
The inner water gap (the region between the square fuel lattice and the channel box wall) and the channel box wall are homogenized into regions with volume averaged cross sections. The spectrum of the homogenized region is set equal to the spectrum of the coolant of the corner pin cell.

Outer water gap
The spectrum of the outer water gap is set equal to the spectrum of the coolant of the corner pin cell.

Control blade
The pin cell spectrum of an absorber rod is calculated the same way as any non-fuel pin, where each non-fuel region is treated as a unique material ring. An additional region between the outermost region and buffer zone is added containing the outer water gap cross sections.

Water wing
The water wing is homogenized with volume averaged cross sections and given the spectrum of the coolant of the corner pin cell.

Explicit detector
The pin cell spectrum of the explicit detector is calculated the same way as any non-fuel pin, where each non-fuel region is treated as a unique material ring. An additional region between the outermost region and buffer zone is added containing the outer water gap cross sections.

15-2. The plenum is considered to be a non-fuel pin. The plenum pin cell spectrum is calculated the same way as a fuel pin, as described in Section 2.3.1 of the Methodology LTR, except that the homogenized plenum material is placed in the fuel region. The material composition of plena is explicitly specified through input by the user. No features are needed to address the very low density of the gas.

**RAI 16: Control Blade and Channel Box Two-Dimensional Coupling**

The NRC staff requires additional details regarding the two-dimensional coupling calculation in terms of the treatment of the control blade and the channel box.

16-1. The channel box is very thin. Is the channel box homogenized with inter- or intra-assembly water?

16-2. If so, does this introduce any appreciable error in the calculation of the spectra at or near the channel?

16-3. The control blade may extend into mesh cells such that only a fraction of a mesh cell is filled with part of a control element. How are these cells homogenized?

16-4. Would such homogenization introduce error in the calculation of the contribution of the tips of the control blade to its worth?

**GNF Response to RAI 16**

16-1. In the two-dimensional coupling calculation, the channel box is homogenized with the intra-assembly water gap between the box wall and the first row of pin cells. The homogenization of the channel box is shown in Figure 2-5 of the Model Description LTR.

16-2. Because the channel box is optically thin, the homogenization of the channel box with the intra-assembly water gap does not introduce any appreciable error in the spectral calculations. Because LANCR02 only uses the coupling calculation to condense the flux spectrum from a fine to intermediate energy group structure, and a full transport solution is performed without any homogenization, the overall effect of homogenization in the transmission probability calculation is negligible.

16-3. If any part of the control blade extends into a transmission probability (TPXY) mesh cell, the entire mesh cell is assumed to be controlled. No homogenization between controlled material and moderator is performed at the ends of the control blade. Similarly, if any part of the central hub of the control blade extends into a TPXY mesh cell, the entire mesh cell is considered central hub material.

16-4. No. This approximation does not introduce any appreciable error because the coupling calculation is only used to condense the cross sections from the library group structure to the transport group structure. The final MoC solution is performed using the exact geometry of the control blade without homogenization.

**RAI 17: Calculation of the Angular Dependent Neutron Source**

In the Method of Characteristics solution of the detailed two-dimensional flux distribution, the LTR states that the neutron sources may be calculated using either transport corrected cross-sections or explicit anisotropic scattering.

17-1. Which approach is used in LANCR02?

17-2. Are source neutrons other than prompt or delayed fission neutrons considered (e.g. $(n,2n)$ reactions)?

17-3. Please provide an equation that relates the angular source in any mesh to the local flux and cross-sections consistent with the LANCR02 method. This should consider the differential scattering or double differential scattering cross-section.

17-4. Please provide the source of the scattering matrix (or matrices) used to perform the mesh source calculation.

**GNF Response to RAI 17**

17-1. The anisotropic scattering effects are accounted for by using transport-corrected cross sections. Explicit anisotropic scattering is not implemented in LANCR02. However, there is nothing inherent in the MoC solution that precludes using anisotropic scattering sources.

To clarify that LANCR02 is using anisotropic scattering, the following changes will be made to the Model Description LTR:

- The sentence above Eq. (28) will be revised to state "The multi-group, discrete angle Boltzmann equation with isotropic scattering of the form,"
- A dot product will be added after the first term in Eq. (28)
- The sentence after Eq. (29) will be modified to state "... which is calculated using transport-corrected cross sections."

17-2. Group-dependent sources include fission sources, neutron scattering, and (n,2n) reactions. Internally to LANCR02, the (n,2n) reactions are implemented by including the reaction in the scattering matrix along with a corresponding change in the absorption cross section to maintain neutron balance. Specifically,

$$\hat{\Sigma}_{s,i}^{g'\to g} = \Sigma_{s,i}^{g'\to g} + 2\hat{\Sigma}_{(n,2n),i}^{g'\to g}$$

$$\hat{\Sigma}_{a,i}^{g} = \Sigma_{a,i}^{g} - \sum_{g'} \hat{\Sigma}_{(n,2n),i}^{g'\to g}$$

17-3. The angular source is isotropic in each flat source region. Therefore, the angular source for each group g, mesh i, and angle m, can be specified as the right-hand-side of Eq. (28),

$$Q_{m,i}^{g} = \frac{1}{4\pi}\left[\sum_{g'} \Sigma_{s,i}^{g'\to g}\phi_i^{g'} + \frac{\chi^g}{k}\sum_{g'} \nu\Sigma_{f,i}^{g'}\phi_i^{g'}\right]$$

This equation is only valid for isotropic scattering.

17-4. The scattering matrix (including the (n,2n) terms) is read from the neutron data library and condensed in a manner similar to all other cross sections. The source of the cross sections on the neutron data library is ENDF/B data processed by NJOY.

**RAI 18: Volume Preservation**

Please provide figures that are substantially similar to the figures provided in slides 11 and 12 of the LANCER pre-submittal meeting held at NRC headquarters in November 2008.

Please incorporate this information in a revision to the LANCR02 Model Description LTR.

**GNF Response to RAI 18**

The following figures are from the presentation given at the LANCR02 pre-submittal meeting held at NRC headquarters in November 2008.

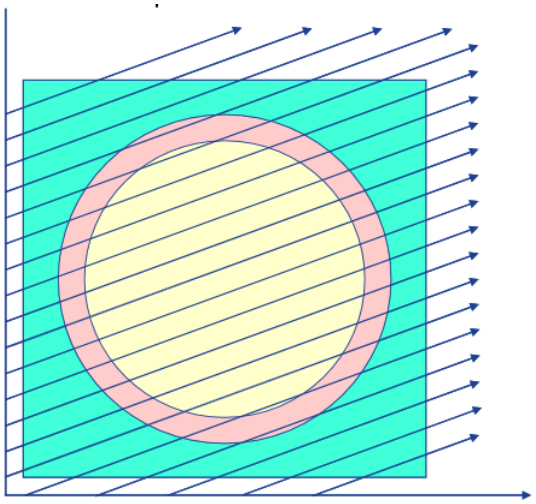

From Slide 11:

Tracks are traced over the entire geometry of the problem at equidistant intervals.

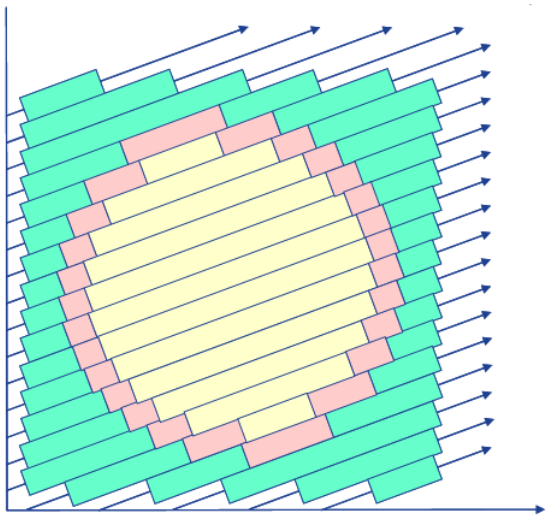

From Slide 12:

The ray tracing generates an approximation to the area of each mesh.

The code independently calculates the true area of each irregular mesh in the problem Track lengths are adjusted slightly to re-produce the true area of each mesh in the problem.

Section 3.3 of the Model Description LTR (“Preserving Mesh Volume”) will be revised to include the figures from these two slides (or substantially similar figures) as Figures 3-3 and 3-4 of the LTR.

**RAI 19: Energy Dependent Azimuthal Angles**

19-1. When the azimuthal directions are adjusted for perfect reflection, are the weights associated with the angles updated?

19-2. If not, please describe those aspects of the method that ensure this does not introduce appreciable error.

19-3. Please provide the standard production energy dependent number of azimuthal directions.

19-4. Considering that the staff requested additional information in another RAI regarding the double-differential cross section, when downscattering occurs how are the different azimuthal separations and associated weights partitioned to model anisotropic scattering where the energy loss results in a change in energy group?

19-5. Please provide an assessment of the validity of any assumptions that are made to model the process of anistropic downscatter.

19-6. The LTR appears to indicate that this azimuthal energy dependent quadrature may be [[ ]] How is the adequacy of the azimuthal quadrature confirmed to be acceptable on [[ ]]?

Please incorporate this information in a revision to the model description LTR.

**GNF Response to RAI 19**

19-1. Yes. When the azimuthal directions are adjusted for perfect reflection, the weights associated with the angles are updated.

The default weight is given by

$$\omega_i = \frac{2\pi}{N_a}$$

as described in Section 3.1.1 in the LTR. More generally, the weight is

$$\omega_i = \begin{cases} \dfrac{\frac{1}{2}\left(\varphi_2 + \varphi_1\right)}{2\pi} \text{ for } i = 1 \\ \dfrac{\frac{1}{2}\left(\varphi_{i+1} - \varphi_{i-1}\right)}{2\pi} \text{ for } i = 1 < i < N_a \\ \dfrac{2\pi - \frac{1}{2}\left(\varphi_{N_a} + \varphi_{N_a-1}\right)}{2\pi} \text{ for } i = N_a \end{cases}$$

for arbitrarily spaced angles.

19-2. When the azimuthal directions are adjusted for perfect reflection, the weights associated with the angles are updated. Therefore, no error is introduced.

19-3. The following table lists the standard production energy dependent number of azimuthal directions:

| **Energy** | **No. Azimuthal Angles** |
|---|---|
| [[ | |
| | |
| | ]] |

19-4. Anisotropic scattering is not currently implemented in LANCR02, and, as such, double-differential scattering does not apply.

19-5. Anisotropic scattering is not currently implemented in LANCR02.

19-6. The number of azimuthal angles can be input into the code. However, a default number of azimuthal angles exists in the code and this default value is used for all production cases. A single set of default values is in the code (see response to RAI 19-3) and is not problem-specific.

The following paragraph from Section 3.1.1 of the Methodology LTR will be modified as

Original
[[

]]

Modified

[[

]]

**RAI 20: Polar Quadrature**

The LANCR02 Model Description LTR is not clear regarding the polar quadrature sets. In particular, the NRC staff cannot determine which of the available quadrature sets is the [[ ]] set.

20-1. The LTR states that three optimal quadrature sets are specified in LANCR02 as being available to the user. Are all three of these sets generated using the optimization method of Tabuchi-Yamamoto where they vary in polar order?

20-2. The LTR states that the Legendre quadrature sets come directly from Reference 13 of the LANCR02 Model Description LTR. Does this refer specifically to the $P_N$ Quadrature Sets?

20-3. The LTR states that the [[
]] quadrature. Please specify what these angles and weights are. Please incorporate this information in a revision to the LANCR02 Model Description LTR.

20-4. Please describe how these were determined (either Tabuchi-Yamamoto optimization, Nth order Legendre polynomial approximation, or by some other method).

20-5. The LTR states that results using the [[
]]. Please demonstrate this assertion.

**GNF Response to RAI 20**

20-1. The three optimal quadrature sets available in LANCR02 are the Tabuchi-Yamamoto quadrature sets that vary in polar order.

20-2. Yes, this refers specifically to the $P_N$ quadrature set. These values are taken from Table 3-1, p. 121 of Reference 13 of the LANCR02 Model Description LTR.

20-3. The Tabuchi-Yamamoto quadrature sets are:

**Table 3-1: Tabuchi-Yamamoto Quadrature Sets**

| Polar Divisions | sin theta | omega (w) |
|---|---|---|
| 1 | 0.798184 | 1.000000 |
| 2 | 0.363900<br>0.899900 | 0.212854<br>0.787146 |
| 3 | 0.166648<br>0.537707<br>0.932954 | 0.046233<br>0.283619<br>0.670148 |

The table of the Tabuchi-Yamamoto quadrature set will be added to Section 3.1.2 of the Model Description LTR.

20-4. The derivation of the Tabuchi-Yamamoto quadrature sets is described in detail in the following reference:

A. Yamamoto, M. Tabuchi, N. Sugimura, T. Ushio, and M. Mori, "Derivation of Optimum Polar Angle Quadrature Set for the Method of Characteristics Based on Approximation Error for the Bickley Function," Journal of Nuclear Science and Technology, Vol. 44, No. 2, p. 129-136 (2007). (Available on-line)

Because the above reference is a more detailed description from a refereed journal, the Model Description LTR will be revised to replace Reference 15 with the reference given above.

20-5. Four lattices are evaluated for this demonstration:

1. GE14 0% void uncontrolled
2. GE14 100% void uncontrolled
3. GE11 MOX 100% void uncontrolled
4. GE11 MOX 100% void controlled

Each lattice is run with 1, 2, 3, 4, 5, and 6 polar angles using the Legendre quadrature set, and 1, 2, and 3 polar angles with the Tabuchi-Yamamoto (TY) quadrature set. Comparisons of k-infinity and pin-by-pin fission density are made against the saturated case (6 Legendre polar angles). The comparisons below show convergence to the saturated result, demonstrating that the Tabuchi-Yamamoto quadrature set produces results near the saturation result.

In the tables below, the eigenvalue difference is given by

$$\Delta k = k_1 - k_0$$

where $k_0 =$ saturated result eigenvalue, and $k_1 =$ eigenvalue generated with the alternate polar set. The pin fission rate (for pin n) is

$$P^n, \text{ where } AVE\left(P^n\right) = 0$$

The difference in the pin-by-pin fission rate density is expressed as a RMS (%) between the quadrature set of interest and the reference (saturated) quadrature set:

$$\text{Pin RMS } = \sqrt{\frac{1}{N}\sum_n \left(P_1^n - P_2^n\right)^2}$$

– Results –

GE14 0% void uncontrolled –

| Legendre | KINF | Δk | pin RMS (%) |
|---|---|---|---|
| [[ | | | ]] |

| TY | KINF | Δk | pin RMS (%) |
|---|---|---|---|
| [[ | | | ]] |

GE14 100% void uncontrolled –

| Legendre | KINF | Δk | pin RMS (%) |
|---|---|---|---|
| [[ | | | ]] |

| TY | KINF | Δk | pin RMS (%) |
|---|---|---|---|
| [[ | | | ]] |

GE11 MOX 100% void uncontrolled –

| Legendre | KINF | Δk | pin RMS (%) |
|---|---|---|---|
| [[ | | | |
| | | | ]] |
| **TY** | **KINF** | **Δk** | **pin RMS (%)** |
| [[ | | | |
| | | | ]] |

GE11 MOX 100% void controlled –

| Legendre | KINF | Δk | pin RMS (%) |
|---|---|---|---|
| [[ | | | |
| | | | ]] |
| **TB2** | **KINF** | **Δk** | **pin RMS (%)** |
| [[ | | | |
| | | | ]] |

**RAI 21: Cold Shutdown Margin Cross-sections**

21-1. When using LANCR02-generated data to perform downstream shutdown margin calculations, how are the bladed cross-sections determined? In particular, the fundamental mode calculation adjusts the radial power distribution to deplete the lattice in a "critical" manner.

21-2. Under cold shutdown conditions the reactor should be in subcritical condition, and the fundamental mode adjustment to the power shape for determining the nuclear parameters may introduce a bias because the flux shape is artificially adjusted. Please describe how nuclear data are calculated to perform cold shutdown evaluations.

**GNF Response to RAI 21**

21-1. The purpose of the fundamental mode calculation is to correct the spectral effects of depleting in an infinite lattice instead of a core-wide (i.e., critical) spectrum. The spectral effects are due to higher energy neutrons having a longer mean-free-path than thermal neutrons. In LANCR02, the fundamental mode calculation is implemented as a 0-D calculation that operates on volume-averaged group fluxes and cross sections. Because the calculation is 0-D, the calculation does not have a direct effect on the radial power within the lattice.

The fundamental mode calculation, described in Section 2.5 of the Model Description LTR, is applied to both controlled and uncontrolled cross sections. There is no special treatment of controlled cross sections in the fundamental mode calculation.

21-2. As implemented in LANCR02, the fundamental mode calculation is a spectral calculation (0-D) and does not have a direct effect on the radial flux shape within the lattice. Other methods (not used in LANCR02) implement a leakage term in the 2-D calculation and this would affect the radial flux shape.

**RAI 22: Cold Calculations**

When determining nuclear parameters to perform cold calculations, how are moderator temperature effects taken into account?

**GNF Response to RAI 22**

Moderator temperature effects are reflected in the scattering cross sections of the fine-group library, which includes the thermal scattering cross section data for bound material moderators (i.e., chemical binding effects) (See RAI 2-2). The moderator temperature is used to interpolate the temperature dependent moderator cross sections at the user defined statepoint.

**RAI 23: Fundamental Mode Adjoint Flux**

Equation (47) appears to be in error. The staff would expect (47) to read as:

$$\overline{\Sigma}_r^g \Psi^{+g} = \sum_{g' \neq g} \overline{\Sigma}_s^{g \to g'} \Psi^{+g'} + \nu \overline{\Sigma}_f^g \sum_{g'} \chi^{g'} \Psi^{+g'}$$

Please explain Equation (47)

**GNF Response to RAI 23**

The Staff is correct that Equation (47) is in error. Equation (41) of the updated Methodology LTR will be replaced by

$$\overline{\Sigma}_r^g \Psi^{+g} = \sum_{g' \neq g} \overline{\Sigma}_s^{g \to g'} \Psi^{+g'} + \nu \overline{\Sigma}_f^g \sum_{g'} \chi^{g'} \Psi^{+g'}$$

**RAI 24: Prompt and Delayed Spectra**

Equations (45) and (46) indicate that an averaged spectrum is used to perform the adjoint weighting. Please provide some clarifying details.

24-1. The prompt and delayed spectra appear isotope independent. If so, please justify this approximation.

24-2. The equations include a bar over a fission spectrum symbol in the equations. The staff takes this to be an average quantity. It appears to be the spectrum for the total fission yield (prompt + delayed). Is this the case?

24-3. When LANCR02 is performing the calculation, does it perform the integration based on the prompt and delayed spectra as shown in the first portion of Equation (45) or (46) or is the calculation based on the second portion of the equations?

24-4. What does the superscript "j" denote?

24-5. The staff assumes that subscript "γ" denotes delayed. Please confirm.

**GNF Response to RAI 24**

24-1. Equation (45) of the LTR is incorrect. The isotope dependence of the prompt fission spectrum is incorporated by calculating region dependent prompt fission spectra, which use isotope dependent prompt fission spectra. The region dependent prompt fission spectra are then lattice averaged over volume, flux, and fission, and normalized to one (1.0) over energy. The delayed spectrum is isotope dependent. Equation (39) in the updated LTR will be replaced with

$$\beta_{eff}^{j} = \frac{\sum_{iso}\left[\beta_{iso}^{j}\left(\sum_{g}\overline{\chi}_{d,iso}^{g,j}\Psi^{\dagger g}\right)\left(\sum_{g}\nu\overline{\sigma}_{f,iso}^{g}\overline{N}_{iso}\Psi^{g}\right)\right]}{\sum_{iso}\left[\left\{\left(1-\sum_{i=1}^{6}\beta_{iso}^{i}\right)\cdot\sum_{g}\overline{\chi}_{p}^{g}\Psi^{\dagger g}+\sum_{i=1}^{6}\left(\beta_{iso}^{i}\left(\sum_{g}\overline{\chi}_{d,iso}^{g,i}\Psi^{\dagger g}\right)\right)\right\}\left\{\sum_{g}\nu\overline{\Sigma}_{f,iso}^{g}\Psi^{g}\right\}\right]}$$

$$= \frac{\sum_{iso}\left[\beta_{iso}^{j}\left(\sum_{g}\overline{\chi}_{d,iso}^{g,j}\Psi^{\dagger g}\right)\left(\sum_{g}\nu\overline{\sigma}_{f,iso}^{g}\overline{N}_{iso}\Psi^{g}\right)\right]}{\sum_{g}\overline{\chi}^{g}\Psi^{\dagger g}\cdot\sum_{g}\nu\overline{\Sigma}_{f}^{g}\Psi^{g}}$$

The subscript indication for delayed has been changed in this equation from "γ" to "d" to distinguish it from the same notation used elsewhere in the Methodology LTR for "gamma". The remainder of the Methodology LTR is unaffected by this notation change and requires no related change.

24-2. Yes, chi bar is used to indicate the total fission spectrum for the homogeneous system.

24-3. The calculation is based on the first part of the equation in RAI response 24-1.

24-4. The superscript “j” represents a delayed neutron group, as indicated following the equation in the LTR.

24-5. The staff is correct. The subscript “γ“ denotes delayed, and this notation has been altered as denoted in RAI response 24-1.

**RAI 25: Power Calculation**

Please provide clarification regarding the power calculation.

25-1. When calculating the kinetic energy deposited from epithermal neutron capture, the calculation is performed using a multi-group calculation, how is the neutron energy treated?

25-2. What is the source of the beta energy release data? Please incorporate this information in a revision to the model description LTR.

25-3. Please describe how heat deposition factors are determined. For example, neutron slowing down energy deposition in the coolant. The LTR states that this calculation is not part of the gamma transport and gamma heat deposition calculation.

25-4. Does LANCR02 consider/calculate heat deposition in spacers?

**GNF Response to RAI 25**

25-1. The kinetic energy deposited from epithermal neutron capture is not treated in LANCR02 as it has been considered and was found to be insignificant compared to fission and gamma energy releases.

25-2. LANCR02 data libraries are consistent with the beta energy release data extracted from the ENDF/B-VII decay libraries. In order to describe better where these values come from, the data are now literally extracted from the ENDF/B-VII decay libraries and have been shown to not have changed any of the values in the Qualification LTR. The model description LTR will be revised to document the current source of the beta energy release data.

25-3. A description of how heat deposition factors are determined is provided in GNF response to RAI 32-5.

25-4. No, LANCR02P does not calculate heat deposition in spacers if material is not explicitly included in the lattice modeling.

**RAI 26: Instrumentation Model**

26-1. Please provide a comprehensive description of the application of the detailed instrument model in LANCR02.

26-2. Using the detailed approach and simplified J-factor approach, provide a comparison of the models to demonstrate the relative efficacy of these two approaches. Please consider typical and modern instrument designs (i.e. thermal TIP, gamma TIP, and gamma thermometers).

26-3. Is the detailed instrumentation model capable of accounting for spacer effects on gamma instrument signals?

**GNF Response to RAI 26**

26-1. This response complements Section 7.5 of the Methodology LTR. The following clarifies the sense of the use of the term “explicit” in the LTR.

[[

]]

26-2. [[

]]

[[

]]

**Figure 26.1: Relative Differences as a Function of Lattice Exposure for the Thermal TIP Model (explicit minus default model); IV stands for instantaneous void fraction**

[[

]]

**Figure 26.2: Relative Differences as a Function of Lattice Exposure for the Gamma TIP Model (explicit minus default model); IV stands for instantaneous void fraction**

[[

]]

**Figure 26.3: Relative Differences as a Function of Lattice Exposure for the Gamma Thermometer Model (explicit minus default model); IV stands for instantaneous void fraction**

26-3. Within the context of modeling spacers with a 2-D model, the detailed and phantom instrumentation models are capable of accounting for spacer effects. However, a complete accounting for spacer effects is a 3-D problem, which is not considered to be within the scope of the LANCR02 methodology.

**RAI 27: Depletion Chains**

The staff requires additional characterization of the depletion chains.

27-1. Are figures 5-1 through 5-4 comprehensive?

27-2. To assist the staff in its review of these chains, please provide a comparison of the LANCR02 chains to the TGBLA06 chains.

**GNF Response to RAI 27**

27-1. The chains in Figures 5-1 through 5-4 are comprehensive and include over 160 isotopes. Note that, as indicated in the response of RAI 2, only PFP2 is shown in the figures. The residual isotopes represented by the pseudo fission products in LANCR02 have negligible reactivity effects and are therefore assigned zero cross sections.

27-2. Two fission product models are available within TGBLA06. The base fission product model consists of 29 major fission products (fission products and their daughters with significant neutron absorption), two gadolinium product isotopes, one gadolinium tail product, 6 zero cross section transition isotopes, and one pseudo fission product representing the contribution from the other minor fission products. The expanded fission product model consists of 40 major fission products (fission products and their daughters with significant neutron absorption), two gadolinium tail isotopes, one gadolinium tail product, 5 zero cross section transition isotopes, and one pseudo fission product representing the contribution from the other minor fission products.

The pseudo fission product in both TGBLA06 models is assigned an effective absorption cross section to capture the effect of the minor fission products.

A comparison between the number of isotopes in TGBLA06 and LANCR02 is shown in the following table:

| | TGBLA06 (Expanded Model) | LANCR02 |
|---|---|---|
| Actinides | 25 | 38 |
| Fission Products | 40 | 125 |
| Other | 8 | 10 |
| Pseudo Fission Product | 1 | 2 |

**RAI 28: Dual Time Step**

28-1. Please specify in greater detail the conditions where the dual time step model is deactivated.

28-2. Please provide specific details as to how LANCR02 will treat lattices with "split" gadolinia loadings, for example, a lattice that includes fuel pins with two different concentrations of gadolinia burnable poison.

**GNF Response to RAI 28**

28-1. The conditions for usage of the dual time step model are determined at a coarse region level, with each coarse region containing a fuel rod and surrounding interstitial space. Each fuel rod of the problem that is "burnable" is determined to be a "Normal rod" when both of the following criteria are met:

$$\frac{N_{Gd155} + N_{Gd157}}{V} < 5.10^{-8} cm^{-3} \text{ and } \frac{N_{Gd157}}{\left\langle \frac{S_{Gd157}}{R_{Gd157}} \right\rangle} \leq 1.25\ cm^{-3}$$

where $N_{Gd155}$ = total number of Gd-155 nuclei per unit length within a coarse region

$N_{Gd157}$ = total number of Gd-157 nuclei per unit length within a coarse region

$V$ = volume per unit length of node ($cm^2$)

$S_{Gd157}$ = production rate of Gd-157

$R_{Gd157}$ = removal rate of Gd-157

and $\langle\ \rangle$ indicates volume ($cm^2$) averaged within sub-regions of coarse region.

Every fuel rod is determined to be either a "Gad rod" or a "Normal rod" according to the stated criteria. If any rod is determined to be a "Gad rod," the entire lattice is treated with the dual time step model. Corollary: If and only if all nodes satisfy the above criteria, the dual time step model is turned off.

28-2. Every fuel rod is determined to be either a "Gad rod" or a "Normal rod" according to the criteria provided in RAI response 28-1. If any rod is determined to be a "Gad rod," the entire lattice is treated with the dual time step model.

**RAI 29: Control Blade Depletion**

How is the control blade depletion model used?

**GNF Response to RAI 29**

The LANCR02 Model Description LTR describes how fuel, burnable absorbers, and control blade regions can be depleted. The currently approved steady-state and transient models used at GNF do not use control blade depletion in the physics solution. Any application of the control blade depletion model to steady-state or transient calculations will be described in future LTR's.

The LANCR02 Model Description LTR also describes how the control blade depletion model can be applied to control blade lifetime calculations. Any approval to use LANCR02 for control blade worth calculations would be the subject of a future NRC submittal.

**RAI 30: Gamma Sources**

Please clarify that the fission gamma sources include the effect of delayed gamma emission.

**GNF Response to RAI 30**

Fission gamma sources include both delayed and prompt gamma emission.

After Eq. (43) in Section 2.6 of the updated Model Description LTR, the following sentence will be added to clarify the source terms: “Fission gamma sources include both delayed and prompt gamma emission.”

**RAI 31: Convergence**

31-1. Please specify the convergence criteria used in the qualification analyses.

31-2. Please specify whether or not the convergence criteria are internal to the LANCR02 code or specified through user input.

31-3. Does user guidance exist for the selection of appropriate convergence criteria if these values are input on a problem-specific basis?

31-4. Please provide any user guidance to this effect including any available guidance in the LANCR02 user manual.

31-5. If maximal limits are established, either internal to the code or through administrative controls, how do these limits compare to those employed for the qualification analysis.

31-6. If maximal convergence criteria limits have not been established, please establish such limits to be used in standard production cases. If the established limits are greater than those used in the qualification analyses, please demonstrate that the accuracy of the results, throughout the range of the applicability of LANCR02, is not unreasonably affected.

**GNF Response to RAI 31**

31-1. The qualification analysis uses the default convergence criteria which is denoted by $\varepsilon$ in Sections 3.6.1, 3.6.2, and 3.6.3 of the Methodology LTR, and has the numerical value of 0.00005.

31-2. Default values of the convergence criteria exist in the code, but the option to override the values by user input should still be considered acceptable. This default convergence criterion was used for all qualification cases, demonstrating that the default values are robust for production work.

31-3. A single set of default convergence criteria exists in the code and this set is not problem-specific. These default criteria may change according to Section 9 of the Methodology LTR.

31-4. No user guidance exists except that the user should use the default values.

31-5. No maximal limits are established for the convergence criteria. All qualification cases were run with the default convergence criteria.

31-6. It is intended that standard production cases will use the default convergence criteria consistent with the value used in the qualification analyses. If it is needed to use a convergence criteria greater than those used in the qualification analysis, a demonstration would be needed to show that the accuracy is not unreasonably affected throughout the range of applicability of the LANCR02 qualification basis over which the convergence criteria are applied. This is consistent with the guidance suggested in the last paragraph of Section 9.2 of the Methodology LTR and the last sentence of the first paragraph of Section 9.3 of the Methodology LTR.

**RAI 32: Code Output**

Please provide the following clarifying details regarding the LANCR02 code output.

32-1. When determining the flux discontinuity factors, is the lattice flux solution utilized based on the leakage corrected flux?

32-2. The listing of code output includes a term "BDC." These appear to be boundary diffusion coefficients. What is the purpose for generating these parameters?

32-3. The CDFNW calculation refers to the southwest corner. The LTR states that LANCR02 is not limited to diagonally symmetric lattices, but discontinuity factors would be required for the northeast corner. Is this output not listed in the LTR?

32-4. Please provide equations for the FLUX1 and FLUX1C outputs. Please incorporate this information in a revision to the model description LTR.

32-5. Please provide the LANCR02 output descriptions that provide heat deposition factors in fuel bundle structures (spacers, cladding, channels, and water rods) and heat deposition factors for the coolant. Please incorporate this information in a revision to the model description LTR.

**GNF Response to RAI 32**

32-1. The flux discontinuity factors are based on the flux solution calculated before the leakage correction. As described in RAI 21-2 response, the fundamental mode calculation, as implemented in LANCR02, is a spectral calculation (0-D) and does not have a direct effect on the radial flux shape within the lattice. Other methods (not used in LANCR02) implement a leakage term in the 2-D calculation and this would affect the radial flux shape.

32-2. The code output "BDC" contains the boundary diffusion coefficients. These factors are not currently used in downstream applications. However, they are made available.

32-3. The staff is correct that the expression for the northeast corner is mistakenly not included in the LTR. LANCR02 is not limited to diagonally symmetric lattices. The following will be added to Section 8.3:

**CDFWN : few-group flux discontinuity factor for wide-narrow (WN) corner**

$$CDFWN(g) = \frac{\psi(g, s = WN)}{\frac{1}{V_{ass}} \int_{V_{ass}} \phi(g, r) dr}$$

where $\psi(g, s = WN)$ is the few-group surface scalar flux in the northeast (Wide-Narrow) corner of the problem. For diagonally symmetric lattices, this will also be the flux in the southwest corner of the problem. (LANCR02 is not limited to diagonally symmetric lattices.)

The following will be added to Section 8.2:

WN = Wide-Narrow gap

32-4. In providing a response to this RAI, GNF has identified that the equation for FFXR in the Methodology LTR is incorrect.

The following will be added to Section 8.2:

$V_{clad}$ = total volume of all clad

Additionally, Section 8.3 of the LTR will be modified to include the following definitions:

**FLUX1 : lattice-averaged fast flux (above 1 MeV)**

$$FLUX1 = FFXR \cdot FNF$$

**FLUX1C : fast flux (above 1 MeV) in the cladding of rod (x,y)**

$$FLUX1C(I,J) = FNF \cdot \frac{\left(\frac{1}{\int_{V_{clad}} dr}\right)\int_{V_{clad}} \phi(E > 1\ \text{MeV})dr}{\left(\frac{1}{\int_{V_{ass}} dr}\right)\int_{V_{ass}} \phi(E > E_2)dr}$$

where $E_2$ is the upper boundary of the 2nd coarse mesh energy group (see Table A-4).

**FFXR : fast flux fraction above 1 MeV**

$$FFXR = \frac{\left(\frac{1}{\int_{V_{ass}} dr}\right)\int_{V_{ass}} \phi(E > 1\ \text{MeV})dr}{\left(\frac{1}{\int_{V_{ass}} dr}\right)\int_{V_{ass}} \phi(E > E_2)dr}$$

where $E_2$ is the upper boundary of the 2nd coarse mesh energy group (see Table A-4).

32-5. The heat deposition factors in fuel bundle structures (cladding, channels, and water rods) and heat deposition factors for the coolant are calculated separately for gamma and neutron slowing down heating. The calculation of the gamma heating is described by Equation (45) of Section 2.6.1 of the updated Methodology LTR.

The following description of heat deposition factors in internal structures from neutron slowing down will be added to Section 8.3 of the Methodology LTR:

**MEVPF: Heat deposition factors in internal structures from neutron slowing down (MeV per fission)**

The energy deposition due to neutron slowing down in region m, Qm, is given by

$$Q_m = \frac{\sum_{g=1}^{G}\sum_{g'=g+1}^{G}\left(E_g - E_{g'}\right)\int_{V_m} N(r)\sigma_s(g \to g',r)\phi(g,r)dr}{\sum_{g=1}^{G}\int_{V_m} N(r)\sigma_f^g(r)\phi(g,r)dr}$$

where Eg = midpoint energy for energy group g (where Eg' < Eg when g' > g), G=number of energy groups, $N(r)\sigma_s(g \to g',r)$ is the macroscopic scattering cross section from group g to g' at r, $N(r)\sigma_f^g(r)$ is the macroscopic fission cross section in group g at r, Φ(g,r) is the g-group fundamental mode leakage corrected flux at r, and Vm is the volume of region m. The energy deposition calculated with the equation is summed for each region type (cladding, channels, and water rods), providing heat deposition factors for neutron slowing down. The gamma energy deposition is treated separately, as described in Equation (51) of the LTR. Therefore, the gamma energy deposition factors calculation does not include the energy deposition from slowing down of neutrons.

Energy deposition due to neutron slowing down is a function of flux and atomic number densities, which are exposure dependent, and therefore atomic number densities and flux are updated accordingly.

1. Total energy deposited in coolant, gap, fuel, channel and additional coolant on the edge rods:
$$E_{All-Lattice} \equiv \sum_{j \in All-Lattice}\left[Q_j\right]$$
2. Energy deposited in coolant (in-channel water, excluding rods water):
$$E_{COO} \equiv \sum_{j \in COO}\left[Q_j\right]$$
3. Energy deposited in gap (out-channel, wings and rods water):
$$E_{MOD} \equiv \sum_{j \in MOD}\left[Q_j\right]$$
4. Energy deposited in fuel:
$$E_{FUE} \equiv \sum_{j \in FUE}\left[Q_j\right]$$
5. Energy deposited in channel:
$$E_{\{BOX,CAN\}} \equiv \sum_{j \in \{BOX,CAN\}}\left[Q_j\right]$$
6. Energy deposited in additional structure such as coolant on the edge rods.
$$E_{rest} \equiv E_{All-Lattice} - E_{COO} - E_{MOD} - E_{FUE} - E_{\{BOX,CAN\}}$$

LANCR02 does not provide the heat deposited in spacers because they are not explicitly modeled as part of the lattice. Heat deposition in bundle structures due to gamma energy deposition is described in Section 2.6.1.

**RAI 33: Model Updates**

33-1. [[

]] however, such capability could be applied to an expanded application scope – which would require NRC review and approval. An example may be [[

]] In these instances the predictive capabilities of the code are being relied upon for an application purpose that is beyond the scope of the staff's current review. Please update this section of the LTR to state that [[

]]

33-2. In terms of model updates to implement the LANCR02 transport solutions [[ ]] without NRC review and approval, the staff requires clarification on this proposed model update. The staff cannot presume the [[

]] would have to be implemented. This type of change would be considered by the staff a departure from the approved method that would require review and approval. However, the staff has some degree of assurance that [[

]]
Revise the model description LTR to include a requirement that when LANCR02 is updated to [[

]]

**GNF Response to RAI 33**

33-1. [[

]] Therefore, GNF believes that the means by which the LANCR02 results will be used in downstream applications and safety analyses is beyond the scope of the current LANCR02 two-dimensional lattice physics model description review.

33-2. Section 9 of the model description LTR will be revised to include the requirement:

"[[

]]”

**RAI 34: Empirical Tuning**

34-1. Please provide descriptive details of any "corrective models" in the LANCR02 method. Here "corrective models" refers to adjustment factors or additional terms that are applied within the base methodology to tune calculated results to match more accurate transport calculations. An example may be adjusting water rod cross sections internal to the code to fit the slowing down power in water rods to more accurate predictions of water rod slowing down using higher order transport methods.

34-2. TGBLA06 included several of these types of models, please address how the analogous phenomena are addressed in LANCR02. At a minimum please address the following:

- [[

]]

**GNF Response to RAI 34**

34-1. LANCR02 uses no "corrective models." The Method of Characteristics treatment is a high accuracy method that solves the transport equation exactly along each characteristic, and so does not require empirical adjustment factors.

34-2. The LANCR02 methodology is entirely dissociated from the TGBLA06 methodology. As such, each of the corrections and adjustments listed by the staff are irrelevant to the LANCR02 methodology.

**RAI 35: Water Cross Specific Questions**

35-1. Relative to the fuel assembly designs with water rods or water boxes, it would appear that significant geometric approximations are made for water crosses. These approximations may introduce errors in the analysis of these geometries that would not be apparent in the analysis of designs with water rods or water boxes. Please provide a complete list of the geometric approximations that are made in order for LANCR02 to model the water wing fuel design geometry. Please justify each of these. Where possible, please provide some quantitative basis to demonstrate the magnitude of the error introduced into the analysis, otherwise provide a qualitative basis. Compare these errors to typical values for biases and uncertainties derived from the comprehensive qualification.

35-2. Please provide details of the two-dimensional coupling calculation as it is applied to water-cross lattices. In particular please address the treatment of the diamond and wings in the homogenization process of the cell results. Section 7.4.2 does not describe the water wings of the water cross design. Please provide a detailed description, including equations, that describes how LANCR02 approximates and analyzes these geometries.

35-3. Please describe how the sub-bundle void distribution model is executed for water cross designs.

35-4. Please describe how the out-of-channel flow area for water cross designs is calculated. Please also provide details of how the UWR parameter is calculated.

**GNF Response to RAI 35**

35-1. The following approximations are made in the LANCR02 geometry of the water cross:

1) The central water diamond is approximated as a central water box, preserving volume of material components.
2) The water wings in LANCR02 are approximated as rectangular, preserving volume of material components, without the exact detail of the design basis.

The errors introduced by these approximations are precisely quantified in Section 5.6 of the Qualification LTR, because the MCNP geometric model, against which LANCR02 results are compared, does include the geometric detail of the design basis with respect to the water diamond and the water wing geometries.

35-2. The two-dimensional coupling calculation, described in Section 2.3.2 of the Methodology LTR, begins by dividing the lattice modeled into a number of non-uniformly spaced Cartesian zones. The number of Cartesian zones depends on whether a gap exists between the fuel array and the edge of the lattice (region containing film thickness between fuel array and inside channel box, channel box, out-channel, and control blade), whether the water wing exists, and whether a control blade is present. The number of Cartesian zones is IN x IN, where

IN = IM + IMADD + NICH

where IM = fuel lattice dimension (e.g., 10)
IMADD= NCOP + 2*IGAP + 2*IBOX
NICH = 1 if water wing present | 0 otherwise.
NCOP = 1 if control blade present | 0 otherwise
IGAP = 1 if gap present | 0 otherwise
IBOX = 1 if channel box present | 0 otherwise

Each Cartesian zone, R, contains a number of regions, each with a unique material composition, flux, and cross section.

The homogenization, described in paragraph 2 of Section 2.3.2, is a simple volume-flux weighted homogenization for each of the Cartesian zones:

$$\Sigma_{x,R}(E) = \int_{V_R} \phi(r,E)\Sigma_x(r,E)dr$$

35-3. There is no special void distribution treatment for water cross designs. This is justified by the fact that the thermal resistance of a higher powered, higher void, sub-bundle is higher, and therefore the void distribution behaves similarly to the bundle without in-channel flow barriers. The method for distributing void within the lattice is described in detail in Section 6 of the Methodology LTR.

35-4. The out-of-channel flow area for water cross designs is calculated the same as it is for other designs,

$A_{out} = A_{lat} – A_{in} – A_{box}$

where $A_{lat}$ = total area of lattice
$A_{in}$ = area inside channel box
$A_{box}$ = area of channel box.

The UWR parameter is calculated as described in Section 8.3 of the Methodology LTR:

UWR = FLODAT(8) / RHOB

where RHOB : reference water density (g/cc) = 0.73749
FLODAT(8) = density of water in water rods (g/cm3)

The density of the water in the water rods is calculated using the liquid and steam densities and void fraction of the out-channel water, by default, although this can be changed through user input.

## MODEL QUALIFICATION NEDC-33377P, REVISION 1 RAIs

### RAI 36: Standard Production and Qualification Analyses

Please clarify what user-selected options in LANCR02 were utilized for the qualification calculations provided in the qualification LTR (NEDC-33377P, Revision 1, "LANCR02 Lattice Physics Model Qualification Report"). Examples may include the number of parallel rays or the power density used for the depletion. If there are differences between the options selected for the qualification analyses and standard production analyses, please provide justification for the differences.

### GNF Response to RAI 36

The qualification test cases in Chapter 5 and 6 of the Qualification LTR generally use options that would be found in "standard production" analysis cases at GNF. Exceptions to this are:

- Unless otherwise stated, all hot test suites are run at a fuel temperature of 560°C. Standard production cases currently use a hot fuel temperature of 475°C for 10x10 lattices and 520°C for 9x9 lattices, which are average fuel temperatures consistent with the power density of depletion. Such a difference has no meaningful effect on the comparisons to MCNP calculations, but merely facilitates the ability to compare. The temperature/power density is a function of lattice and application in any event and all values are within the application range of LANCR02.
- All test suites use an infinite spectrum option (no buckling correction). Standard production cases perform a leakage correction to the cross sections. The leakage correction was not used in the test suites because there is no equivalent option available in MCNP.
- All test suites use a uniform void distribution. Standard production cases currently use a distributed void option. The distributed void option was not used in the test suites because there is no equivalent option available in MCNP.
- The hot test cases in the test suite use void points at 0, 40, 80, and 100%. These are representative cases that span the in-channel void range, but are not necessarily those that are required by the 3D core simulator application.

In addition, the qualification test cases in Chapter 6 use an internal code option to calculate the energy per fission in a manner that is consistent with MONTEBURNS. In standard production cases, the energy per fission is calculated from models that are not available in MONTEBURNS.

Also, for the qualification test cases in Chapter 6, smaller depletion steps are used in LANCR02 than are normally used in standard production cases. The reason for this change is to maintain consistency with the MONTEBURNS depletions.

**RAI 37: Doppler Coefficient**

While "CDOP" is used to calculate the Doppler coefficient, and is representative of the change in lattice reactivity with temperature, it is not technically the Doppler coefficient. Rather, it is a parameter that characterizes the Doppler coefficient (see Equation 10 of NEDO-20964-A). Please reconcile this inconsistency and update the qualification LTR.

**GNF Response to RAI 37**

In the Qualification LTR (NEDC-33377P, Revision 1), the Doppler coefficient is defined as:

$$CDOP = \frac{k(T_{HI}) - k(T_{LOW})}{(\sqrt{T_{HI}} - \sqrt{T_{LOW}})k(T_{LOW})}$$

In NEDO-20964-A, this same quantity is defined as the "[Doppler] constant of proportionality". This quantity (CDOP) is calculated by the lattice physics code and is used in the core simulator to calculate the Doppler reactivity coefficient. The Doppler reactivity coefficient in core simulators is defined as the derivative with respect to the fuel temperature instead of the derivative with respect to the square root of the fuel temperature.

The definition of CDOP in Section 2 of the Qualification LTR will be changed to define CDOP as the "Doppler Constant of Proportionality" and state that this quantity is used to calculate the Doppler coefficient in core simulators. Where applicable, the remainder of the Qualification LTR will be revised to change "Doppler Coefficient" to "CDOP".

**RAI 38: "W/F"**

The NRC staff assumes that "W/F" refers to the water to fuel ratio. This ratio as provided in Table 4.4-1 does not agree with the moderator to fuel volume ratio provided in the International Handbook, September 2008 edition. Please reconcile this inconsistency and update the qualification LTR to define "W/F".

**GNF Response to RAI 38**

For the benchmark experiments taken from LEU-COMP-THERM-006, the Water-to-Fuel (W/F) ratios reported in the LANCR02 Qualification LTR are identical to those reported in the International Handbook September 2008 edition.

For all other benchmark experiments, the W/F ratios were calculated using the following equation(s):

$$W/F = \frac{A_w}{A_F} = \frac{A_{unitcell} - A_{fuel}}{A_{fuel}} = \frac{A_{unitcell}}{A_{fuel}} - 1$$

$$A_{unicell} = LatticePitch^2$$

$$A_{fuel} = \pi R_{fuel}^{\ 2}$$

Section 4.4.2 of the LANCR02 Qualification LTR will be revised to include these definitions.

**RAI 39: MCNP Light Water Reactor Critical Benchmarks**

Please provide Reference 8: NEDO-32028, “MCNP: Light Water Reactor Critical Benchmarks,” dated March 1992.

**GNF Response to RAI 39**

Section 2.6 of NEDO-32028 pertains to the LANCR02 critical benchmarks in Section 4.1 of NEDC-33377P, Revision 1. Section 2.6 and supporting figures from the 1992 report are included herein. Please note that the terminology used for test is different between the LANCR02 LTR and the old report. The test called “Jersey Central Experiments” in LANCR02 is equivalent to the “Small Core Critical with and without Poison Curtains” in the 1992 report.

| Isotope | ORNL-1 | ORNL-2 |
|---|---|---|
| H-1 | 6.62280e-2 | 6.61480e-2 |
| O-16 | 3.37360e-2 | 3.38000e-2 |
| N-14 | 1.86900e-4 | 2.12900e-4 |
| U-234 | 5.38000e-7 | 6.31000e-7 |
| U-235 | 4.80660e-5 | 5.62060e-5 |
| U-236 | 1.38000e-7 | 1.63000e-7 |
| U-238 | 2.80700e-6 | 3.28100e-6 |
| B-10 | --- | 1.02860e-6 |

## 2.5 The PNL Plutonium Nitrate Solution Experiments

The two PNL experiments[7,8] examined in this study consisted of reflected spheres of radius 19.5085 cm (this radius was derived from a quoted critical volume of 31.1 liters). The atom densities of the various isotopes are given below in units of atoms/barn-cm at room temperature:

| Isotope | PNL-1 | PNL-2 |
|---|---|---|
| H-1 | 6.563e-2 | 5.416e-2 |
| O-16 | 3.456e-2 | 3.977e-2 |
| N-14 | 6.216e-4 | 4.720e-3 |
| Pu-239 | 9.373e-5 | 4.141e-4 |
| Pu-240 | 4.501e-6 | 1.988e-5 |

## 2.6 The Small Core Critical With and Without Poison Curtains

This experiment had a core of fuel bundles arranged in a 4x4 configuration. The bundles contained fuel rods set up in a 7x7 matrix. In one case, the four central bundles were surrounded by borated stainless steel curtains; the other had no curtains. Both cores were simulated in a full three-dimensional configuration with water reflectors radially as well as below the active fuel region. The fuel bundles and, where applicable, the poison curtains extended beyond the active fuel region to a total height of 365 cm from the plane corresponding to the bottom of the active fuel. The reflector region

below the active fuel extended 38 cm and contained water. The active fuel region contained water and the region above the active fuel region contained no moderator. The total core height in both the cases was 403 cm. Criticality was achieved by varying the water level in the core.

Figure 2.1 shows the core with one-eighth symmetry and Figure 2.2 shows the bundle dimensions and spacings. Three features shown in Figure 2.2 have not been used in the Monte Carlo model: (1) the rounded corners shown for the bundles have been replaced in the model with right angle corners; (2) the dished fuel rods (with a lower fuel density) have not been treated separately (instead, a properly weighted average density was used for all fuel); and (3) the spacer material is not included in the model. None of these approximations is likely to affect a global parameter like the effective multiplication factor, though local quantities like fission density could be affected. The reflecting boundaries are marked in Figure 2.1.

The fuel rods were also modeled without the gap between the fuel and the cladding. The fuel densities quoted below are the densities smeared into the gap. The outer radius of the fuel rod was 0.7239 cm and the radius of the smeared fuel was 0.63373 cm. The clad material was Zircaloy-2. The density of water in the experiment was quoted as being 0.99254 g/cc.

The isotopic compositions of the three fuel types are as follows:

| | Atom Densities in atoms/barn-cm | | |
|---|---|---|---|
| Fuel | U-235 | U-238 | O-16 |
| High Enrichment 2.42 w% - $U^{235}$ | 5.36816e-4 | 2.13722e-2 | 4.38181e-2 |
| Intermediate Enrichment 1.67 w% - $U^{235}$ | 3.70452e-4 | 2.15368e-2 | 4.38145e-2 |
| Low Enrichment 1.19 w% - $U^{235}$ | 2.63968e-4 | 2.16421e-2 | 4.38121e-2 |

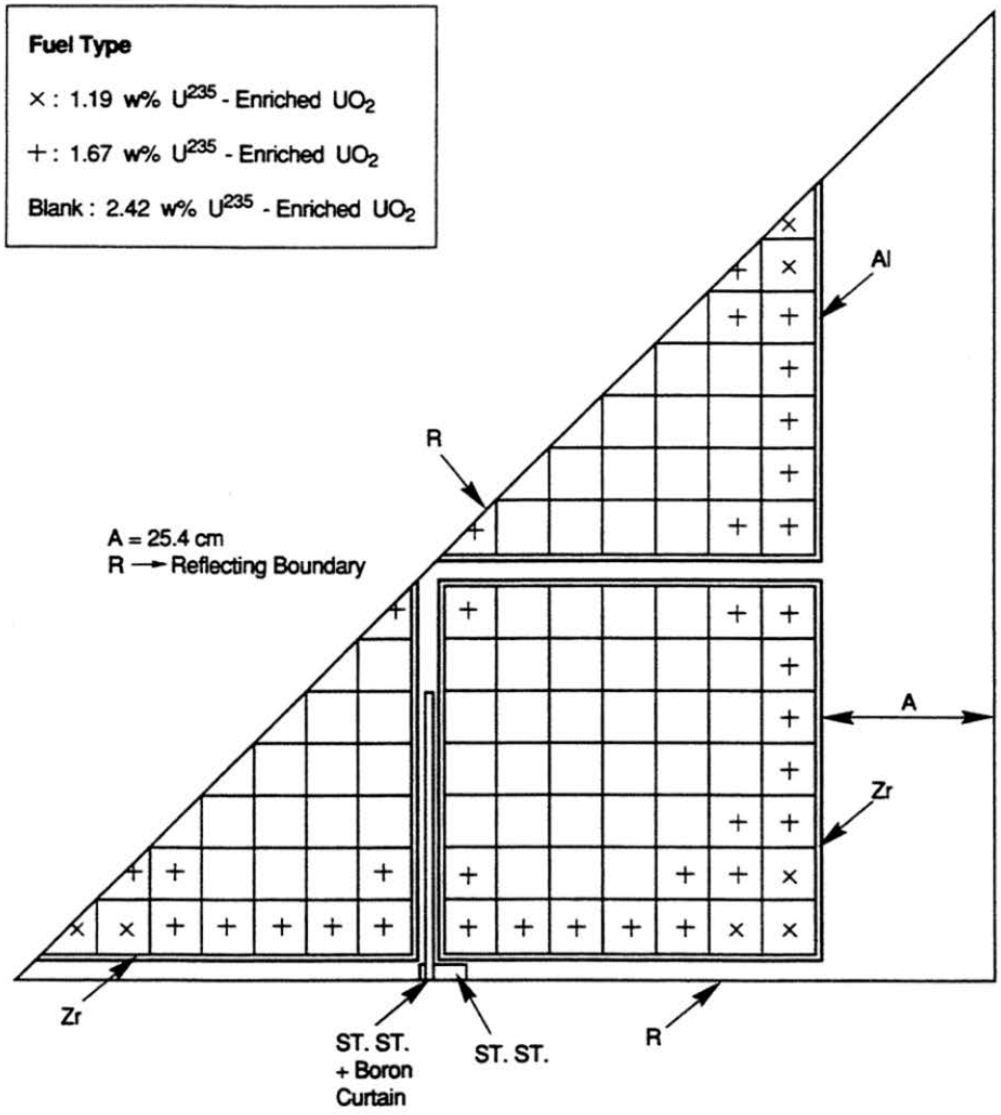


Figure 2.1 Small Core Critical With Poison Curtains:
One Eighth Core Symmetry

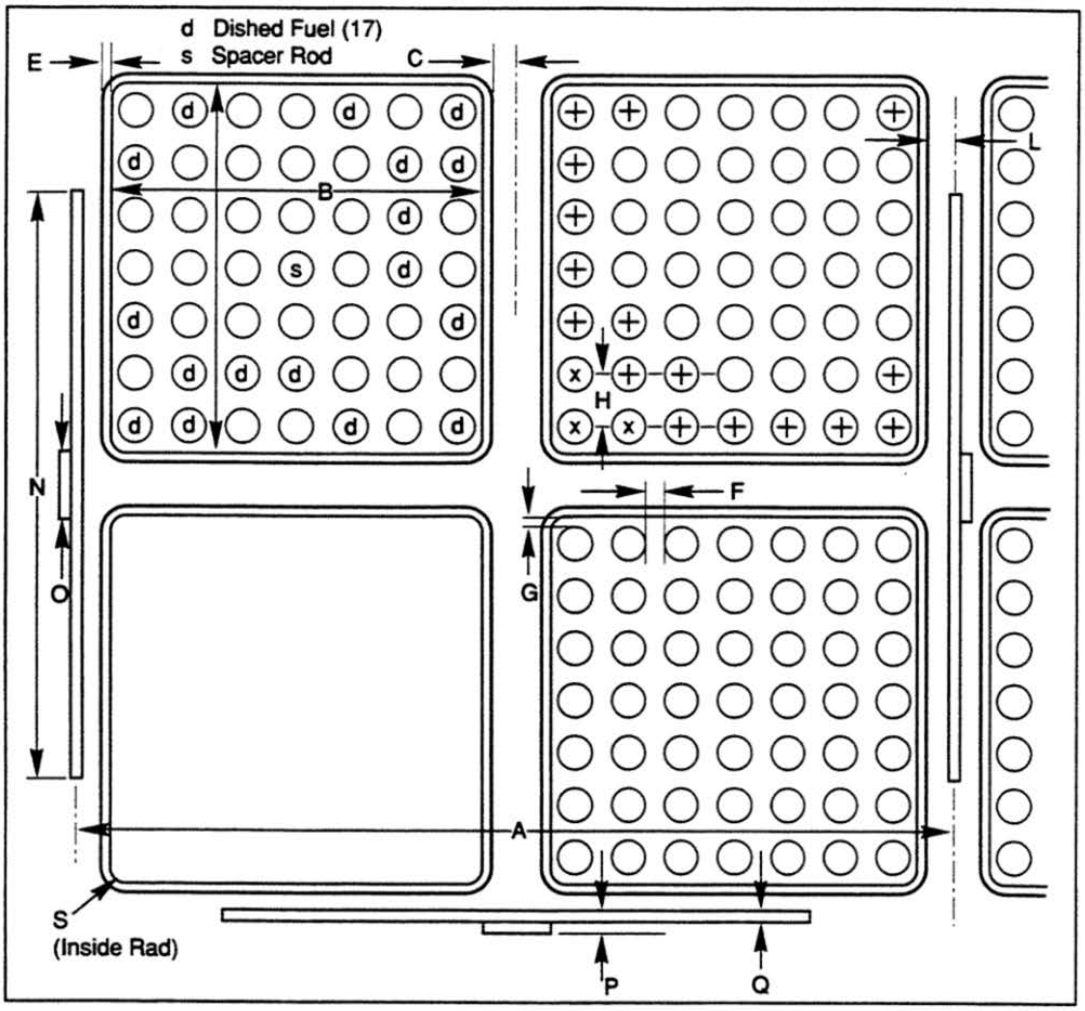


All dimensions are in cm.

| | |
|---|---|
| A = 30.48 | L = 0.47498 |
| B = 13.40612 | N = 21.4376 |
| C = 0.9525 | O = 1.42748 |
| E = 0.2032 | P = 1.42748 |
| F = 0.42672 | Q = 0.19304 |
| G = 0.3556 | S = 1.016 |
| H = 1.87452 | |

Figure 2.2 Small Core Critical With Poison Curtains: Bundle Configuration

The Zircaloy-2 had an atomic density of 4.3333e-2 atoms/barn-cm and the following composition in atom fractions:

| | |
|---|---|
| Natural Zr | 9.76712e-1 |
| Tin | 1.14803e-2* |
| Iron | 2.27730e-3 |
| Chromium | 2.09647e-3 |
| Nickel | 6.19150e-4 |
| O-16 | 6.81491e-3 |

The aluminum channel had an atom density of 6.02612e-2 atoms/barn-cm.

The small core with poison curtains had a critical height of 175.49 cm. The poison curtains and the stainless steel stiffeners (Figures 2.1 and 2.2) had the following composition:

| | Atom Densities in atoms/barn-cm | |
|---|---|---|
| Isotope | Curtain | Stiffener |
| Iron | 5.855690e-2 | 5.87802e-2 |
| Nickel | 8.121020e-3 | 8.15200e-3 |
| Chromium | 1.624210e-2 | 1.63040e-2 |
| Silicon | 8.548450e-4 | 8.58105e-4 |
| Mn-55 | 1.709690e-3 | 1.71621e-3 |
| B-10 | 3.306597e-4 | --- |
| B-11 | 1.330950e-3 | --- |

The small core without the poison curtains had a critical height of 55.07 cm.

## 2.7 The Small Core Critical With Burnable Absorbers

This set of experiments, which was performed outside the General Electric Company, consisted of fuel bundles arranged in a 4x4 matrix configuration. The fuel bundles had rods arranged in an 8x8 matrix with some rods being poisoned with $Gd_2O_3$. The moderator was water with

---

*The cross sections for this element were processed from the ENDL-73 library.

**RAI 40: MCNP Results for LWR Critical Benchmarks**

There appear to be minor inconsistencies with the Monte Carlo N Particle (MCNP) results reported in the International Handbook and the Global Nuclear Fuel (GNF) MCNP results for several cases (LEU-COMP-THERM-001, -002, -006, and -039) when the same cross section libraries are referenced (Evaluated Nuclear Data File B-VII.0 (ENDF/B-VII.0)). Please reconcile.

**GNF Response to RAI 40**

The cases where the International Handbook reports results using ENDF/B-VII are:

1. LEU-COMP-THERM-001 (cases 1-4)
2. LEU-COMP-THERM-002 (cases 1-5)
3. LEU-COMP-THERM-006 (cases 1-18)
4. LEU-COMP-THERM-039 (cases 1-4 and 7-10)

The table below shows the average $K_{eff}$ and standard deviation for these cases for the International Handbook and GNF results:

| | International Handbook | GNF |
|---|---|---|
| Average $K_{eff}$ | 0.999297 | 0.999730 |
| Average standard deviation of $K_{eff}$ | 0.000103 | 0.000347 |

The difference between the average $K_{eff}$ is minimal and found to be 0.000436. This difference can be attributed to the following reasons:

1. The number of particles (and/or cycles) used in the International Handbook results is more than that used in GNF. This is observed by the higher standard deviation in the GNF results.
2. The Thermal S(α,β) Cross-Section Libraries for Hydrogen in Light Water and for Hydrogen in Polyethylene are evaluated at 300 $^{o}$K in the International Handbook results and at 293 $^{o}$K (for light water) and 296 $^{o}$K (for polyethylene) in the GNF results.

The importance and relative effect of the differences stated above will vary from one case to another.

**RAI 41: Test Suite Perturbations**

For completeness, please specify the lattice-type analyzed (C-, N-, S-, or D-) and the control blade design in the description of the test suites in the qualification LTR.

**GNF Response to RAI 41**

The following table lists the lattice-types and control blades used in the test suites of Chapters 5 and 6 of the Qualification LTR. If the descriptions are not already included in the test suite descriptions, the Qualification LTR will be updated to add the descriptions.

| Test Suite Number | Lattice Type | Control Blade | New text to be added to test suite description (if applicable) |
|---|---|---|---|
| 1 | C | D100 | N/A |
| 2 | C, D, or N (as indicated by lattice number in Table 5.2-3) | D100 | N/A |
| 3 | C | D100 | N/A |
| 4 | C | D100 | "All bundles are analyzed for a C-lattice plant containing a D100 control blade." |
| 5 | C | D100 | "All bundles are analyzed for a C-lattice plant containing a D100 control blade." |
| 6 | Alternate Product Lines | D100 | "These lattices are non-GNF designs. The 9x9 lattice has asymmetric gaps. The 10x10 lattices have symmetric gaps." |
| 7 | C | D100 | "All bundles are analyzed for a C-lattice plant containing a D100 control blade." |
| 8 | C | D100 | "All bundles are analyzed for a C-lattice plant containing a D100 control blade." |
| 9 | C | D100 | "The lattice analyzed is for a C-lattice plant containing a D100 control blade." |
| 10 | C | D100 | "All bundles are analyzed for a C-lattice plant containing a D100 control blade." |
| 11 | C and D (as indicated by blade type in Table 5.11-2) | various | "All bundles are analyzed for a C-lattice, except for the cases for blade type D230, which corresponds to a D-lattice type." |
| 12 | C | D100 | "The lattice analyzed is for a C-lattice plant containing a D100 control blade." |
| 13 | C | D100 | "The lattice analyzed is for a C-lattice plant containing a D100 control blade." |
| 14 | C | D100 | "The lattice analyzed is based on that for a C-lattice plant containing a D100 control blade." |
| 15 | C | D100 | "The lattice analyzed is for a C-lattice plant containing a D100 control blade." |
| 16 | C | D100 | "The lattice analyzed is for a C-lattice plant containing a D100 control blade." |
| 17 | C | D100 | "All bundles are analyzed for a C-lattice plant containing a D100 control blade." |
| Chap 6 | C | D100 | "The lattice analyzed is for a C-lattice plant containing a D100 control blade." |

**RAI 42: Mixed Oxide Test Suite**

The mixed oxide (MOX) suite does not consider gadolinia-bearing MOX fuel rods. Is this a limitation for LANCR02?

**GNF Response to RAI 41**

There is no technical limitation in LANCR02 for modeling this accurately, but the option for gadolinia-bearing MOX fuel rods is not required at this time because there are no plans to manufacture gadolinia-bearing MOX fuel rods for BWR's. Approval for modeling gadolinia in MOX fuel rods is not requested in LANCR02.

**RAI 43: Reactivity Worth of Depleted Lattice Test Suite**

43-1. Please describe the process by which depleted fuel compositions are determined for the MCNP calculations.

43-2. Table 5.5-16 appears to be inconsistent with the LTR text in Section 5.5.7. Please reconcile this inconsistency.

**GNF Response to RAI 43**

43-1. The process for calculating the depleted fuel conditions in Test suite 5 is to deplete a lattice in LANCR02 to the specified exposure step. At that point, the nuclide densities calculated by LANCR02 are used to create a consistent MCNP input deck. The purpose of the test suite is to compare LANCR02 and MCNP results for a consistent set of isotopes at exposed conditions. All other test suites in Chapter 5 are at zero exposure.

43-2. The text in Section 5.5.7 is inconsistent with Table 5.5-16. The text above Table 5.5-16 in the Qualification LTR will be updated to state [[

]]

**RAI 44: Gadolinia Loading**

44-1. To provide the staff with reasonable assurance in the capability of LANCR02 to simulate the depletion of gadolinium using the standard two-step approach, please supplement the Depletion Test Suite (Section 6) with a comparison of gadolinium-155 and gadolinium-157 pin-wise inventory between LANCR02 and MONTEBURNS.

44-2. Please supplement test suite 7 with some cases at alternative temperatures to compare the Doppler reactivity predictions.

44-3. Please supplement test suite 7 with some controlled cases to compare the control rod worth predictions.

**GNF Response to RAI 44**

44-1. The response to RAI 44-1 is a comparison of gadolinium-155 (Gd-155) and gadolinium-157 (Gd-157) concentrations in selected pins of a representative lattice up to the point of Gadolinia burnout, or where the Gadolina concentration is less than 1% of the initial concentration. The pin-wise inventories were compared between MCNP6 and LANCR02 results. MCNP6 was used in place of MONTEBURNS due to its ability to provide the user with pin-wise isotopic data in a straightforward way.

**Code System Description**

In the LANCR02P Qualification LTR and Depletion Test Suite 6, MONTEBURNS was used as an alternate calculation to validate LANCR02's burnup capability; however, it is not straightforward to extract pin-isotopic information from this previous analysis. Instead, the more state-of-the-art Monte Carlo depletion methods available in MCNP6 (specifically MCNP 6.1.1 Beta) were leveraged in this evaluation.

MCNP6 is a Los Alamos National Laboratory (LANL) Monte Carlo transport code which combines the functionality of previous versions of the code, MCNP5 and MCNPX, as well as some additional features. MCNP is an industry standard code that can be used to calculate eigenvalues for fissile systems using continuous-energy Monte Carlo radiation-transport. The geometry of a complex three dimensional system can be described in Cartesian coordinates by a collection of bounded surfaces.

Depletion with KCODE is one significant advantage of MCNP6 over MCNP5, or MCNP-05P, the GEH/GNF production version of the code. In MCNP6, steady-state flux calculations are performed followed by nuclide depletion calculations in the CINDER90 subroutine. The concentration of each nuclide is then updated for each specified material before the steady-state flux calculations are repeated for the next time step. Isotopes on the user-defined material cards and specified in the selected fission product tier are included in the steady-state particle transport. Additionally, those produced by the isotope generator as daughters of default and user-specified isotopes are included in the steady-state particle transport. MCNP6 reports the material-wise isotopic data to the user for each time step.

This depletion method in MCNP6 is distinct from that used by MONTEBURNS, which is an automation tool that couples MCNP with the burnup code ORIGEN2. The principal

function of MONTEBURNS is to provide ORIGEN2 with 1-group cross sections from MCNP, and then pass depleted isotopic information back to MCNP5.

In order to evaluate the consistency between the new alternate calculation tool (MCNP6) and the original method (MONTEBURNS), an eigenvalue comparison was performed. The results are shown in Figure 44-1.1 and demonstrate all three codes have excellent agreement. This provides confidence that the depletion results presented in Test Suite 6 remain valid while allowing new investigation into pin-specific fuel inventories to be performed with the more modern, user friendly tool.
[[

]]

**Figure 44-1.1: Eigenvalue Comparisons at 40% Void Fraction**

**Selected Lattice**

[[

]]

**Table 44-1.1: Selected Fuel Pins and Their Composition**

| Pin | Concentration (wt%) U-235 | Gadolinia |
|---|---|---|
| [[ | | ]] |

[[

]]

**Figure 44-1.2: Selected Fuel Pins**

**Results**

The depletion of Gd-157 at 40% void fraction was analyzed as the percent of initial Gd-157 concentration. A 40% void fraction was chosen as it is representative of a typical depletion case. Equation 44-1.1 shows the calculation, where $C_{initial}$ is the initial concentration of Gd-157 and $C_{\exp}$ is the concentration of Gd-157 at a specific exposure step.

$$\%Initial = \frac{C_{\exp}}{C_{initial}} \qquad (44\text{-}1.1)$$

[[

]]

[[ ]] (44-1.2)

[[

]]

**Table 44-1.2: Maximum Absolute Difference of Percent Initial Concentration at 40% Void Fraction**

| Pin | Gd-157 | Gd-155 |
|---|---|---|
| [[ | | |
| | | ]] |

Gad-157 Comparisons

[[

]]

**Figure 44-1.3: Difference of Percent Initial Gd-157 in the** [[
]]

[[

]]

**Figure 44-1.4: Difference of Percent Initial Gd-157 in the** [[
]]

[[

]]

**Figure 44-1.5: Difference of Percent Initial Gd-157 in the** [[
]]

[[

]]

**Figure 44-1.6: Difference of Percent Initial Gd-157 in the** [[
]]

Gad-155 Comparisons

[[

]]

**Figure 44-1.7: Difference of Percent Initial Gd-155 in the** [[
]]

[[

]]

**Figure 44-1.8: Difference of Percent Initial Gd-155 in the** [[
]]

[[

]]

**Figure 44-1.9: Difference of Percent Initial Gd-155 in the** [[
]]

[[

]]

**Figure 44-1.10: Difference of Percent Initial Gd-155 in the** [[
]]

44-2. Test Suite 7 has been supplemented to include some cases at elevated fuel temperatures to compare the Doppler reactivity predictions. The standard BOL, uncontrolled cases at void levels of 0, 40, 80, and 100% of Test Suite 7 will be evaluated at a fuel temperature of 1500°C.

Section 5.7.2 of the Qualification LTR has been revised to reflect the addition of these cases. In addition, two new figures (Figures 5.7-2 and 5.7-3) were added for the hot Doppler eigenvalue differences and the hot controlled eigenvalue differences, respectively. The titles of Figures 5.7-1 and 5.7-4, and 5.7-5 were also revised to clarify that these figures reflect the hot uncontrolled cases.

44-3. Test Suite 7 has been supplemented with additional cases at controlled conditions to compare the control rod worth predictions. The standard BOL, 560°C fuel temperature cases at void levels of 0, 40, 80, and 100% of Test Suite 7 will be evaluated at controlled conditions.

Sections 5.7.3 and 5.7.4 of the Qualification LTR have been revised to reflect the addition of these cases.

**RAI 45: Enrichment Test Suite**

45-1. It is assumed that for each enrichment the void fraction increases from left to right. Please update Figures 5.9-2 and 5.9-3 to distinguish the cases according to void fraction.

45-2. Please provide a pin peaking factor figure similar to Figure 5.1-3 of this LTR.

45-3. There appears to be a typographical error in Section 5.9.5. The maximum eigenvalue error appears to be [[ ]] according to Table 5.9-4.

**GNF Response to RAI 45**

45-1. The independent axis in Figures 5.9-2 and 5.9-3 is the case number. A description of each case number is provided in Table 5.9-3. This table includes a detailed description of each case number, including enrichment, void, and lattice type. From this table, it can be observed that for a given enrichment, the void fraction increases with case number. The figures do not need to be updated in the LTR.

45-2. A figure showing the difference in pin peaking factors is given below as Figure 45-2.1.
[[

]]

**Figure 45-2.1: Difference in Pin Peaking Factor**

45-3. The text in Section 5.9.5 will be modified to reflect the correct maximum eigenvalue error of [[ ]].

**RAI 46: Borated Lattices**

Please confirm that the units of boron concentration are provided in parts per million natural boron equivalent.

**GNF Response to RAI 46**

The units of soluble boron concentration are provided as parts per million natural boron equivalent. Natural boron is assumed to be 19.8 atom% B-10.

**RAI 47: Control Blades**

47-1. Please define the following terms in the qualification LTR: "OEM" and "ABB."

47-2. Please update Figure 5.11-2, 5.11-3, and 5.11-4 to depict the various void fractions. The NRC staff assumes that the void fraction increases from left to right in these figures.

47-3. The alternative control blade design test suite does not consider cold eigenvalue. The NRC staff notes that other test suites address the variation in reactivity with temperature. Please assist the NRC staff in assessing the capability of LANCR02 to provide cross-section data for cold shutdown margin calculations by providing statistical summary results for the 0 percent void fraction cases.

47-4. It appears there is a trend [[ ]]. Please clarify the LTR text regarding observed trends.

**GNF Response to RAI 47**

47-1. The following text will be added to Section 5.11.2 of the Qualification LTR:

"Original Equipment Manufacturer (OEM) control blade types are conventional B4C control blades comprised of multiple vertical absorber rods contained within a stainless steel sheath. An example of this type of blade is the standard Duralife D100 model. Asea Brown Boveri (ABB) control blade types consist of a solid bar of stainless steel containing horizontal holes filled with B4C."

In addition, Tables 5.11-2 and 5.11-4 of the Qualification LTR will be revised to add the abbreviation "(ABB)", as in "Horizontal B4C holes drilled in a solid bar of SS304 (ABB)"

47-2. Table 5.11-4 provides the relationship of void fraction (%) to case number. As observed, for each control blade type, the void fraction increases with case number. The dependent axis in Figures 5.11-2, 5.11-3, and 5.11-3 is the case number, which is directly related to Table 5.11-4. The figures do not need to be updated.

47-3. For all 0% void fraction cases, the average eigenvalue difference is [[ ]], with a standard deviation of [[ ]]. This is consistent with the 0% void fraction cases and the cold controlled cases from Test Suite 1.

47-4. The Qualification LTR will be revised to add the following text above Table 5.11-5, "[[

]]"

**RAI 48: Channel Bow**

48-1. The channel bow results appear to consider water rod bow within the channel. Has this type of bow been observed?

48-2. The degree of bow considered is 2 millimeters (79 mils). How does this compare with the expected range of bow for current operating plants?

**GNF Response to RAI 48**

48-1. Channel bow refers to deflection of the entire bundle, including channel, fuel rods, and water rod(s), primarily due to non-uniform irradiation growth of the channel itself. Interior spacing of the fuel rods and water rods is preserved for the levels of bow experienced in the BWR fleet. Assumption of a cosine shape with zero deflection at the ends and a center maximum peak is acceptable. For any two-dimensional plane, the deflection results in an increase in the channel-to-channel spacing resulting in an increase in the power peaking around the wider gap. Therefore, this scenario is modeled at the lattice level by shifting the lattice away from the control blade location, effectively only changing the water gap width.

48-2. The channel bow of a bundle will vary during life depending on the location in the core and its operating history. At lower exposures (< 35 GWd/MTU), bow is generally much less than 2 mm. At higher exposures channel bow generally falls in the range of 0 to 5 mm. A deflection of 2 mm provides a reasonable representation for the purposes of demonstrating the accuracy of LANCR02 for typical configurations.

**RAI 49: Fuel Rod Variation**

49-1. Please clarify in the qualification LTR what is meant by [[ ]].

49-2. Please provide the dimensions of the fuel rods in this test suite in the qualification LTR.

**GNF Response to RAI 49**

49-1. The purpose of this test suite is to qualify a non-fuel bearing, non-depletable rod in the lattice. In this test suite, “zirconium rods” refers to solid natural zirconium rods. However, other inert materials, such as stainless steel or Zircaloy, would also be acceptable to use.

49-2. Dimensions of the fuel rods used in each case in Test Suite 15 are summarized below:
[[

]]

**RAI 50: Neutron Balance**

Is the production term for the zirconium isotopes listed in Tables 15.6-3 through 15.6-6 from (n, 2n) reactions?

**GNF Response to RAI 50**

It is assumed that the staff is referring to Tables 5.16-3 and 5.16-6 instead of Tables 15.6-3 and 15.6-6.

Yes, the MCNP production terms include the (n,2n) reaction, but the LANCR02 production terms do not. In LANCR02, the (n,2n) reactions are combined with the scattering matrices, and are therefore not considered separately as a source for the neutron balance results. This approximation results in a small difference in the production source of less than 0.2%.

In answering this RAI, it has been observed that “Zr” should not be included in the following sentence in Section 5.16.4: “Results are not shown for the minor isotopes U-234, Gd-154, Gd-156, Gd-158, Gd-160, O (in the fuel), and Zr.” This sentence in the Qualification LTR will be revised to indicate that Zr is included in the results.

**RAI 51: Infinite vs. Critical Flux weighting**

A study in NUREG-CR-7164 has shown that appreciable error in the calculation of βeff may be introduced when using the formulation in LANCR02. Specifically, the issue arises when using a critically adjusted (fundamental mode/B1) adjoint flux in the calculation of βeff (the approach LANCR02 will use for production cases) rather than an infinite adjoint flux. See NUREG-CR-7164 Section 5 for detailed information. Please provide a comparison of βeff as calculated using an adjoint critical flux weighting and an adjoint infinite flux weighting for both controlled and uncontrolled lattices. Also, please discuss any other differences in the results of LANCR02 that may be introduced by using a critical spectrum as compared to an infinite spectrum.

**GNF Response to RAI 51**

LANCR02 already provides both the critically adjusted adjoint flux and infinite adjoint flux weighted $\beta_{eff}$ values at each state point. Sections 2.5 and 8.3 of the updated Methods LTR will be updated to reflect the availability of both versions of the $\beta_{eff}$ values.

The comparison of the different $\beta_{eff}$ values is shown in Figure 51-1.1 and these values are consistent with the observations made in NUREG-CR-7164. Figure 51-1.1 plots the relative difference in $\beta_{eff}$ (i.e., $(\beta_{eff,HC} - \beta_{eff,HU})/ \beta_{eff,HU}$) against exposure. Each column in the figure represents the delayed neutron energy groups and each row represents the different void fractions.

No changes to LANCR02 are required and the use of either the critical or infinite spectra in the calculation of $\beta_{eff}$ has no effect on the LANCR02 results.

[[

]]

**Figure 51-1.1: Comparison of the Critical and Infinite Adjoint Weighted $\beta_{eff}$ Value**

**RAI 52: Lattice Compositions and Test Suites**

Please provide a summary of the lattice compositions (e.g. Gadolinium loading, fuel enrichment, etc.) used in each of the qualification test suites. If any lattice's composition changes for a specific test suite in the qualification LTR, please indicate these changes in the summary and at the beginning of the corresponding test suite section. Please incorporate this information in a revision to the model qualification LTR.

**GNF Response to RAI 52**

The Qualification LTR will be updated to include the requested information.